CFD STUDY OF SINGLE PHASE FLOW AROUND SPHERICAL PARTICLES

A DISSERTATION

Submitted in partial fulfillment of the requirements for the award of the degree of

MASTER OF TECHNOLOGY

in

CHEMICAL ENGINEERING

(with specialization in Industrial Pollution Abatement)

By

PANKAJ VERMA

DEPARTMENT OF CHEMICAL ENGINEERING
INDIAN INSTITUTE OF TECHNOLOGY ROORKEE
ROORKEE - 247 667 (INDIA)
JUNE, 2007

INDIAN INSTITUTE OF TECHNOLOGY ROORKEE
ROORKEE

CANDIDATE'S DECLARATION

I hereby declare that the work, which is being presented in the dissertation entitled **"CFD STUDY OF SINGLE PHASE FLOW AROUND SPHERICAL PARTICLES"** in the partial fulfillment of the requirements of the award of the degree of Master of Technology in Chemical Engineering with specialization in Industrial Pollution Abatement, submitted in the Department of Chemical Engineering, Indian Institute of Technology Roorkee, Roorkee, is an authentic record of my own work carried out during the period from June 2006 to June 2007 under the supervision of **Dr. Ravindra Bhargava**, Assistant Professor, Department of Chemical Engineering, Indian Institute of Technology Roorkee, Roorkee.

I have not submitted the matter, embodied in this dissertation for the award of any other degree.

Date: 29 June, 2007
Place: Roorkee

(PANKAJ VERMA)

CERTIFICATE

This is to certify that the above statement made by the candidate is correct to the best of my knowledge and belief.

29.6.2007

(Dr. Ravindra Bhargava)
Assistant Professor,
Department of Chemical Engineering,
Indian Institute of Technology Roorkee,
Roorkee - 247667 (India).

ACKNOWLEDGEMENT

I express my deep sense of gratitude to my guide **Dr. Ravindra Bhargava**, Assistant Professor, Department of Chemical Engineering, Indian Institute of Technology Roorkee, Roorkee, for his keen interest, constant guidance and encouragement throughout the course of this work, his experience, assiduity and deep insight of the subject held this work always on a smooth and steady course. Useful criticism and constant help extended in the hours of need had been immensely useful.

Thanks are due to **Dr. Shri Chand**, Professor and Head, Department of Chemical Engineering, Indian Institute of Technology Roorkee, Roorkee, for providing various facilities during this dissertation.

I thank all well wishers who in any manner directly or indirectly have put a helping hand in any part of this piece of work.

Above all, I want to express my heartiest gratitude to all my family members for their love, faith and support for me, which has always been a constant source of inspiration.

PANKAJ VERMA

ABSTRACT

The transport processes occurring around spherical particles is of fundamental importance to numerous scientific fields. An understanding of such phenomena is of relevance to flow phenomena within packed beds typically encountered in chemical reaction engineering, as well as single and multiphase flow phenomena within porous media such as rocks and soil. Packed bed reactors with multiphase flow have been used in a large number of processes in refinery, fine chemicals and biochemical operations. This has prompted extensive studies of mathematical and physical models for these systems.

In this present work a qualitative study of single phase flow around spherical particles has been made. For this study simulations for the laminar model and K-ε model have been carried out using CFD code FLUENT 6.2.16 and results of these simulations have been analyzed.

The system considered for this study is a tubular column of diameter of 30 mm and length of 300 mm. This column consists of six layers of spherical particles of 5 mm diameter. Each layer has four particles at a constant distance of 2 mm and the distance between the layers is also 2 mm. The first layer is placed at a distance of 140 mm from the inlet.

Results obtained from these simulations shows that the 140 mm inlet length is not sufficient for the development of the fully developed flow except for 9.8 m/s of inlet velocity. The velocity between the two adjacent particles is like a jet and low in the remaining part of the packed bed is predicted accurately. Velocity near the wall is found to be of zero value. Pressure fluctuations are high between the wall and the adjacent particles and between the two adjacent particles. The pressure distribution is constant in the rest region of the bed which is free from the influence of the surface boundary of the particles.

Eddy formation is found between the two adjacent particles and the intensity of the is found to be lower in the case of laminar model but in the case of K-ε model the eddies are found to be of higher intensity.

CONTENTS

LIST OF FIGURES

CHAPTER – I

INTRODUCTION

1.1 GENERAL

Describing the transport processes occurring around spherical particles is of fundamental importance to numerous scientific fields, ranging from reservoir engineering to the application of packed beds in chemical processes. Owing to their complexity, porous media are often treated as an effectively homogeneous system from which bulk properties of the flow are determined. This approach neglects the complexity of flow within the individual pores and constrictions which constitute a typical porous medium. Such local information is required to understand and describe completely any given physical process occurring within the system. A commonly encountered situation is that of laminar flow within the porous medium, where viscous effects dominate the transport, this is often referred to as the creeping flow regime. as well as transitions from this creeping flow regime as inertial forces become important as a result of changing flow rate and Reynolds number. An understanding of such phenomena is of relevance to flow phenomena within packed beds typically encountered in chemical reaction engineering, as well as single and multiphase flow phenomena within porous media such as rocks and soil.

Packed bed reactors with multiphase flow have been used in a large number of processes in refinery, fine chemicals and biochemical operations. This has prompted extensive studies of mathematical and physical models for these systems. One of the crucial factors in the study of packed bed systems is the velocity distribution of the flowing fluid across the bed. Various mathematical models of velocity distribution in packed beds have been developed; however, a consensus has not been reached and there is a need for further research in

this area. Packed beds have many industrial applications and are increasingly used in the process industries due to their low pressure drop. With the introduction of more efficient packings, novel packing materials (e.g. adsorbents), new applications (e.g. flue-gas desulphurization) and the trend towards increased capacity plants, the aspect ratio (height: diameter) of such beds is decreasing.

Packed bed reactors belong to the most widely applied reactors, their popularity originating from their effectiveness in terms of performance as well as low capital and operating costs. The reactants flowing through a packed bed reactor can be both in the form of gas or liquid. In numerous applications both phases are present. However, a study of single-phase flow is of particular interest to this work since it is not only essential for single-phase applications, but also constitutes the basis for studying two-phase flow through packed beds.

However, it has to be kept in mind that differently shaped particles also pack with different degrees of bed porosity, which results in different pressure drops as well as different overall bed activities. As a rough rule it is said that the bed porosity increases the more the shape of particles deviates from the spherical shape. This problem can be met to some degree with the use of loading techniques, which give higher bed densities. Obviously, the comparison of efficiency of different particles is not straightforward as the choice of the appropriate shape and size of the catalyst particles as well as the loading technique will be determined by the specific transport and kinetic characteristics of a given process. Two additional criteria, namely the strength of the catalyst particles and their manufacturing cost also need to be taken into account in determining the appropriate particle shape.

The considerations regarding the optimum structure of packed bed reactors are complex, therefore a systematic study is needed if we are to find a model or correlation for predicting single-phase flow pressure drop of any practical value

as no shape and size of particles constituting the packed bed as well as loading technique can be ruled out.

1.2 WHAT IS CFD

Computational fluid dynamics or CFD is the analysis of systems involving fluid flow, heat transfer and associated phenomena such as chemical reactions by means of computer-based simulation. the technique is very powerful and spans a wide range of industrial and non-industrial application areas.

The main reason why CFD has lagged behind is the tremendous complexity of the underlying behaviour, which precludes a description of fluid flows that is at the same time economical and sufficiently complete. The availability of affordable high performance computing hardware and the introduction of user-friendly interfaces have led to a recent upsurge of interest and CFD is poised to make an entry into the wider industrial community. Use of CFD provides several unique advantages over experiment-based approaches to fluid systems design:

- Substantial reduction of lead times and costs of new designs

- Ability to study systems where controlled experiments are difficult or impossible to perform (e.g. very large systems)

- Ability to study systems under hazardous conditions at and beyond their normal performance limits (e.g. safety studies and accident scenarios)

- Practically unlimited level of detail of results

1.3 HOW DOES A CFD CODE WORK

CFD codes are structured around the numerical algorithms that can tackle fluid

flow problems. In order to provide easy access to their solving power all commercial CFD packages include sophisticated user interfaces to input problem parameters and to examine the results. Hence all codes contain three main elements: (i) a pre-processor, (ii) a solver and (iii) a post-processor. Here we briefly examine the function of each of these elements within the context of a CFD code.

1.3.1 Pre-processor

Pre-processing consists of the input of a flow problem to a CFD program by means of an operator-friendly interface and the subsequent transformation of this input into a form suitable for use by the solver. The user activities at the pre-processing stage involve:

- Definition of the geometry of the region of interest: the computational domain
- Grid generation-the sub-division of the domain into a number of smaller, non- overlapping sub-domains: a grid (or mesh) of cells (or control volumes or elements)
- Selection of the physical and chemical phenomena that need to be modeled
- Definition of fluid properties.
- Specification of appropriate boundary conditions at cells which coincide with or touch the domain boundary

1.3.2 Solver

There are three distinct streams of numerical solution techniques: finite difference, finite element and finite volume methods. in outline the numerical methods that form the basis of the solver perform the following steps:

• Approximation of the unknown flow variables by means of simple functions

• Discretisation by substitution of the approximations into the governing flow equations and subsequent mathematical manipulations.

• Solution of the algebraic equations.

The main differences between the three separate streams are associated with the way in which the flow variables are approximated and with the discretisation processes.

The finite volume method was originally developed as a special finite difference formulation. Now it is central to four of the five main commercially available CFD codes: PHOENICS, FLUENT, FL0W3D and STAR-CD.

1.3.3 POST-PROCESSOR

As in pre-processing a huge amount of development work has recently taken place in the post-processing field. Owing to the increased popularity of engineering workstations, many of which have outstanding graphics capabilities, the leading CFD packages are now equipped with versatile data visualisation tools. These include:

• Domain geometry and grid display

• Vector plots

• Line and shaded contour plots

• 2D and 3D surface plots

• Particle tracking

• View manipulation (translation, rotation, scaling etc.)

• Colour postscript output

More recently these facilities may also include animation for dynamic result display and in addition to graphics all codes produce trusty alphanumeric output and have data export facilities for further manipulation external to the code. As in many other branches of CAE the graphics output capabilities of CFD codes have revolutionised the communication of ideas to the non-specialist.

CHAPTER – II

LITERATURE REVIEW

The modeling of single phase flow in packed bed has been carried out by several researchers. For many years the approach for the design of packed bed has been the trial and error method. In this method, the design calculation is performed repeatedly until some restriction on the design parameters is met. The initial guesses must be good ones for this method to converge easily. The literature review is arranged under three categories such as Analytical, Experimental and CFD studies.

2.1 Analytical

Parsons and Porter described a general numerical technique for modeling three-dimensional, single-phase gas flow patterns in packed beds. Specifically, it presented a method for implementing a vectorial form of the well-known Ergun equation in a computational fluid dynamics (CFD) package. The approach is validated by comparison with independent experimental results. The general approach can be used to model flow patterns in adsorbers, catalytic reactors, etc., thus forming a useful design tool whereby packed bed configurations can be designed for minimum pressure drop while avoiding gas maldistribution.

Subagyo et.al. gave a new mathematical model of velocity distribution of single-phase fluid flow in packed beds. The model can be applied for both compressible and incompressible fluids. The validity of the model has been checked using the measured data at inside and downstream of the bed. The agreement between measured data and the results predicted by the model is good.

van Gulijk studied structured packed beds filled with catalyst pellets used for heterogeneous or catalytic reactive distillation. First a simplifying model, the Toblerone model, was developed. This model simplifies the problem of multiphase flow in structured packed beds to single phase flow in intersecting triangular channels. The liquid flow field is solved using the Ergun equation to account for porous flow trough the pellets.

Lesage et.al. they applied the boundary element method to solve highly non-linear differential equations describing hydrodynamics and liquid/solid mass transfer at the wall of a packed-bed reactor with single-phase liquid flow. It is based on the boundary integral element concepts where both the dependent variable and its gradient become the primary variables. Two radial porosity profiles were used to take into account the non-uniformity character of the bed. It was shown that the computed velocity profiles have the same shape as the porosity profiles. The mass transfer experimental measurements, obtained for four different Schmidt numbers, are in good agreement with the computed predictions when uniform velocity profiles are used.

Li et.al. measured the distribution of liquid flow rate in a rectangular bed non-uniformly packed with different particles. The effects of particle properties (size and wettability), liquid properties (viscosity and surface tension) and packed structure on the liquid flow rate distribution were examined. An experimental equation expressing the liquid flow distribution at the interface between different particles is derived by means of the capillary number.

Humby et.al. They reported, for the first time, a systematic comparison of a lattice-gas automata based explicit numerical simulation (ENS) tool for the flow of single-phase fluids in porous media with experiment.

Ortiz-Arroyo and Larachi they developed a Lagrange–Euler–Euler computational fluid dynamic approach to represent the evolution of two-phase pressure gradients in trickle-bed reactors undergoing deposition of colloidal/non-colloidal fines under deep-bed filtration conditions. The simulations were benchmarked using the experimental pressure drop data and observations of Gray, Srinivasan and Masliyah(2002), Pressure build-up in gas–liquid flow through packed beds due to deposition of fine particles.

Changfu et.al. Numerical simulations of flow over a stationary particle in a dense gas-particle two-phase flow were carried out for small Reynolds numbers (less than 100). In order to study the influence of the particles interaction on the drag force, three particle arrangements have been tested: a single particle, two particles placed in the flow direction and many particles located regularly in the flow field.

Larachi et.al. they proposed a computational fluid dynamic methodology to breakdown into elementary dissipation mechanisms for the overall single-phase gas flow bed pressure drop in towers containing corrugated sheet structured packings.

2.2 Experimental

Latifi et.al. presented an experimental and theoretical study of the liquid-to-wall mass transfer in a packed bed reactor with single phase liquid flow. The measurements were carried out by means of the classical electrodiflirsion method and the influence of Schmidt number was particularly investigated. A model based on the division of the packed bed into a core zone and a wall zone was developed.

Johns, Sederman and Gladden Magnetic resonance imaging (MRI) velocity measurement techniques were used to investigate flow of water and a glucose solution within the interparticle space of a cylindrical packed bed of 5 mm

diameter glass ballotini. The experiments were performed over a range of Reynolds numbers from 0.84 to 14.52, spanning the regime where inertial effects begin to play a significant role relative to viscous forces.

Suekane, Yokouchi and Hirai The velocity distributions in a pore that models a simple-packed bed were measured directly by a magnetic resonance imaging technique. With an increase in the Reynolds number from 12.17 to 59.78 - 204.74, the increase and decrease in main flow velocity did not correspond to the local pore geometry, as is the case with a creeping flow. This indicated that inertial forces dominate over viscous forces. For example, at the Reynolds number of 204.74, the fluid penetrated through the center of the pores like a jet with negligible change of velocity. Circulation in the surrounding stagnant spaces generated eight symmetrical eddies in the plane perpendicular to the main flow direction.

Damjan and Levec they studied Single-phase pressure drop in a region of flow rates that is of particular interest to trickle bed reactors ($10<Re<500$). Bed packings were made of uniformly sized spherical and non-spherical particles. Bed porosities in the range of 0.37–0.52 were studied. It was shown that wall effects on pressure drop are negligible as long as the column-to-particle diameter ratio is above 10. Furthermore, the capillary model approach such as the Ergun equation is proven to be a sufficient approximation for typical values of bed porosities encountered in packed bed reactors.

2.3 CFD studies

Jiang et.al. applied a discrete cell model (DCM), based on the minimization of the total rate of energy dissipation, is applied to compute the fluid velocity field in two-dimensional packed beds. The analysis of the individual terms of the energy dissipation rate equation is also presented. The results obtained by DCM are validated both by comparing them with the solutions of CFDLIB code and by available experimental results.

Jiang et.al. understanding the mechanism of flow maldistribution is the first step in avoiding it. In order to achieve this objective, computational fluid dynamic (CFD) simulations of multiphase flow under steady state and unsteady state conditions in bench-scale cylindrical and rectangular packed beds were presented for the first time. The porosity distribution in packed beds is implemented into CFD simulation by pseudo-randomly assigned cell porosity values within certain constraints. The flow simulation results provide valuable information on velocity, pressure, and phase holdup distribution.

Chan et.al. In this work, a detailed k -fluid Eulerian two-dimensional transient computational fluid dynamic (CFD) model has been formulated for the description of the space-time evolution of the clogging patterns developing in deep bed filtration (DBF) of fines'-containing non-aqueous liquids. A local formulation of the macroscopic logarithmic filtration law has been proposed, as well as a geometrical model for the effective specific surface area for momentum exchange. Transient, 2-D axisymmetrical simulations were performed and the approach was benchmarked using the experimental results and observations of Narayan et al. (1997).

Natarajan et.al. their work was concerned with finding out an effective way of eliminating oxygen from a packed bed of monomer particles. This process finds application in industries involved in the manufacture of Nylon12. This work involves the numerical simulation and experimental verification of the flow in a packed bed. In addition, a parametric study is carried out for the parameters such as the number of injectors, the radial position of injectors, and the position of the injectors along the circumference of the packed bed to find out the best possible combination for effective elimination of the oxygen. The packed bed was modeled using a porous medium approach available in the commercial computational fluid dynamics (CFD) software FLUENT.

Higler and Krishna they presented a study of flow in structured packing, whereby main focus is on the liquid flow inside the filled channels. In addition a methodology was presented on how to tackle these novel internal types, so that with a combination of limited experiments and CFD calculations a good impression can be obtained about the contacting characteristics of these packings, and therefore of the possible use and applicability of these new internals. In this paper main focus was on CFD and interpretation of numerical results.

Nijemeisland and Dixon they studied the relationship between the local flow field and the local wall heat flux in a packed bed of spheres. Computational fluid dynamics was used as a tool for obtaining the detailed velocity and temperature fields, for gas flowing through a periodic wall segment test cell.

Gunjal, Ranade and Chaudhari studied fluid flow through the array of spheres using the unit-cell approach, in which different periodically repeating arrangements of particles such were considered. Single-phase flow through these geometries was simulated using computational fluid dynamics (CFD). The model was first validated by comparing predicted results with published experimental and computational results.

CHAPTER – III

MATHEMATICAL MODELING

3.1 GENERAL

Number of researchers have done the mathematical modeling of single phase flow in a packed bed. Different types of systems have been suggested for improving the performance of the packed bed. In this chapter development of a mathematical model is given for the single phase flow in the packed bed.

3.2 Mathematical Development

The main theoretical study of fluid flow in packed beds has been approached in two ways. In the first approach, it is assumed that there is no fluid interaction between voids, similar to fluid flow in a bundle of tangled tubes, i.e. discontinuous system. While in the second approach, it is assumed that the fluid interaction occurs between voids, similar to fluid flow around a collection of submerged objects, i.e. continuous system. Based on the results of macroscopic view, the discontinuous approach has been more successful for packed beds with voidage less than 0.5; and for those with voidage higher than 0.5, the continuous approach is more appropriate. it is appropriate to apply both approaches in developing a mathematical model of velocity distribution in packed beds. The discontinuous approach is applied for the region in which the voidage is lower than 0.5 and for the rest, the continuous approach is used.

For the region in which the voidage is less than 0.5, it is assumed that the fluid flow in a packed bed is similar to fluid flow inside a bundle of tangled tubes with radius *re*. By using a definition of hydraulic radius, r_H then the quantity r_e can be expressed in terms of r_H, as follows:

$$r_e = 2\, r_H \tag{1}$$

where r_H is calculated as follows:

$$r_H = \frac{\varepsilon\, D_p}{6\,(1-\varepsilon)} \tag{2}$$

The mechanical energy balance for fluid flow in a single tube is

$$\int_{p_z}^{p_{z+\Delta z}} \frac{V}{g}\,dp + \frac{1}{2g}\Delta u_z^2 + \Delta Z = -\frac{f_k L u_z^2}{4 g r_e} \tag{3}$$

Equation (3) is applicable for straight pipes with constant diameter and with no heat or work transferred. The concept of equivalent length, Le, for describing fluid flow through non regular piping sections such as bends or sections with changing cross-sectional area. The value of Le is the length of pipe itself plus an equivalent length allowance for non-regular piping sections, so the friction energy losses are equal to the losses in the straight-line pipe of length Le. Considering the fluid flow in packed beds, the value of Le can be defined by the following equation:

$$Le = \xi\, \Delta Z \tag{4}$$

where ξ is a correction factor. Interstitial velocities can be calculated using the following equation which relates the interstitial and the superficial velocity with bed voidage:

$$u_Z = \frac{u_m}{\varepsilon} \tag{5}$$

By assuming that the value of correction factor, ξ, is constant over the cross section of the bed and replacing L in eq. (3) with Le, then substituting eq. (1) into eq. (3) gives

$$\int_{p_z}^{p_{z+\Delta z}} \frac{V}{g} dp + \frac{1}{2g} \Delta u_z^2 + \Delta Z \left(1 + \frac{f_k \xi u_z^2}{8 g r_H} \right) = 0 \qquad (6)$$

If $\Delta z \rightarrow 0$ and using Blake's equation for friction factor, f_k, eq. (6) can be simplified and solved for positive value of u_z:

$$u_z = \frac{-\lambda_2 + \sqrt{\lambda_2^2 - 4\lambda_1 \lambda_3}}{2\lambda_1} \qquad (7)$$

Where

$$\lambda_1 = 1.3125 \frac{(1-\varepsilon)}{\varepsilon} \frac{\rho \varepsilon}{Dp} \qquad (8)$$

$$\lambda_2 = 112.5 \frac{(1-\varepsilon)^2}{\varepsilon} \frac{\mu \xi}{D_p^2} \qquad (9)$$

$$\lambda_3 = \frac{\partial p}{\partial z} + \rho g \qquad (10)$$

The applicability of eqs (7) - (10) is restricted to voidages of less than 0.5. However, in most cases of randomly packed bed systems, the voidage in the region close to the wall is higher than 0.5. Hence, in this case, the above equations are no longer tenable and the continuous approach is more appropriate.

Considering the fluid flowing through a packed bed at the wall region, no-slip condition is assumed at the container wall and $r_{0.5}$, is a radial position in the bed which has voidage equal to 0.5. Employing the momentum balance in the wall region with the local voidage higher than 0.5 and assuming the flow of fluid is only driven by the difference of momentum and the fluid is Newtonian, the following equation can be generated:

$$\frac{\partial}{\partial r}\left(r\varepsilon\frac{\partial u_z}{\partial r}\right)=0 \tag{11}$$

The boundary conditions are

At $r = r_{0.5}$, $\varepsilon = 0.5$, $u_z = ur_{0.5}$ (12)

At $r = R$, $\varepsilon = 1.0$, $u_z = 0$ (13)

Equation (11) with the two boundary conditions, eqs (12) and (13), can be solved by using a polynomial approximation and by assuming that in the region of concern voidage is a linear function of *r*. The minimization of the residual carried out using the collection method, gives

$$u_z = \omega_o + \omega_1 r + \omega_2 r^2 \tag{14}$$

where the coefficients are

$$\omega_o = -R(\omega_1 + \omega_2 R) \tag{15}$$

$$\omega_1 = \frac{5\,r_{0.5} + R}{3\,(r_{0.5} - R)^2}\,u_{r_{0.5}} \tag{16}$$

$$\omega_2 = \frac{u_{r_{0.5}} - \omega_1 (r_{0.5} - R)}{r_{0.5}^2 - R^2} \tag{17}$$

The value of correction factor, m, can be evaluated by using the equations derived from a material balance of the system and assuming steady-state condition as follows:

$$m = \frac{\pi R^2 \rho u_M}{4} \tag{18}$$

and

$$m = 2\pi\rho \int_0^R r\varepsilon u_Z dr \tag{19}$$

Pressure drop in the bed can be evaluated by using the Ergun equation

$$\frac{\Delta p}{L} = 150 \frac{(1-\varepsilon_o)^2}{\varepsilon_o^3} \frac{\mu u_M}{D_p^2} + 1.75 \frac{(1-\varepsilon_o)}{\varepsilon_o^3} \frac{\rho u_M^2}{D_p} \tag{20}$$

The radial voidage distribution of a bed of spherical particles can be calculated by the correlation of Muller:

$$\varepsilon = \varepsilon_b + (1 - \varepsilon_b) J_o(a\hat{r}) e^{-b\hat{r}} \quad \text{for D/Dp >2.02} \tag{21}$$

where

$$a = 7.45 - \frac{3.15}{D/Dp} \quad \text{for 2.02 < D/Dp < 13.0} \tag{22}$$

$$a = 7.45 - \frac{11.25}{D/Dp} \quad \text{for D/Dp > 13.0} \tag{23}$$

$$b = 0.315 - \frac{0.725}{D/Dp} \tag{24}$$

$$\hat{r} = \frac{r}{Dp} \quad \text{for } 0 < r < Dp \tag{24}$$

$$\varepsilon_b = 0.365 + \frac{0.220}{D/Dp} \tag{25}$$

3.2.1 Fluid flow at the downstream of the bed

A velocity distribution at the downstream of the bed is assumed to be a developing flow distribution in an empty pipe with a velocity distribution inside the distribution model is here developed by assuming that there is no-slip at the wall, steady-state condition apply, the fluid is Newtonian with constant density and viscosity, the radial component of the equations of motion is negligible, and any angular motion is negligible (axisymmetric flow). The following equations can be derived from momentum balance and material balance:

$$\rho u_Z \frac{\partial u_Z}{\partial z} = -\left(\frac{\partial p}{\partial z} + \rho g\right) + \mu\left(\frac{1}{r}\frac{\partial}{\partial r}\left(r\frac{\partial u_Z}{\partial r}\right) + \frac{\partial^2 u_Z}{\partial z^2}\right) \tag{26}$$

The boundary conditions are:

$$\text{at } Z = 0, \quad u_Z = u_o \tag{27}$$

$$\text{at } Z = \infty, \quad u_Z = u_\infty \tag{28}$$

The value u_0 is the velocity at the exit of the bed that can be calculated from the velocity distribution inside the bed times the local voidage. The value of u_∞ is the fully developed velocity.

The equations of motion for developing flow have been numerically and analytically solved for many simplified cases. However, all of these solutions used the boundary condition that the velocity at the entrance, u_0, is independent of the radius. This boundary condition is different from that of the

flow at the exit of the bed. Therefore, the solution of the equations of motion with boundary condition as represented in eqs (27) - (28), is needed. Eqs (26) – (28) are transformed to the following dimensionless forms:

$$\frac{d^2\phi}{d\zeta^2} - (\eta_1 + \eta_2\phi)\frac{d\phi}{d\zeta} - \eta_3 = 0 \tag{29}$$

and the boundary conditions become

$$\text{at } \zeta = 0, \quad \text{ø} = 1 \tag{30}$$

$$\text{at } \zeta = R, \quad \text{ø} = 0 \tag{31}$$

where

$$\eta_1 = \frac{N_{Re}\, u_\infty}{2\, u_M} \tag{32}$$

$$\eta_2 = \frac{N_{Re}\,(u_o - u_\infty)}{2\, u_M} \tag{33}$$

$$\eta_3 = \frac{R^2}{\mu(u_o - u_\infty)}\left(\frac{dp}{dz} + \rho g\right) \tag{34}$$

$$\phi = \frac{u_z - u_\infty}{u_o - u_\infty} \tag{35}$$

$$\zeta = \frac{Z}{R} \tag{36}$$

By inspection, it is evident from eqs (29) - (31) that ø is a function of ζ and will be damped out exponentially with ζ. Therefore, ø can be approximated by a function chosen so that all the boundary conditions are exactly satisfied as follows:

$$\text{ø} = e^{-\beta\zeta} \tag{37}$$

The parameter β is a constant to be determined. The parameter β can be represented by the following equation:

for $N_{Re} < 2100$:

$$\beta = 2.41\, N_{Re}^{-0.5} \tag{38}$$

for $N_{Re} > 2100$:

$$\beta = 0.05 \tag{39}$$

CHAPTER – IV

SYSTEM CONFIGURATION

The system used in the present study is consisting of spherical particles in a tubular flow system.

The tubular system has one inlet and one outlet. Water flows into the inlet at a rate of 7.312 mm/s and output works on pressure difference in the range of 2 kPa to 150 kPa.

The tubular system has the diameter of 30 mm and it contains six layers of spherical particles of diameter 5 mm. Each layer consists of four spherical particles. The first layer of spheres is at 140 mm from inlet of the packed bed. The total height of the packing is 40 mm. the space between the spheres is 2 mm and the space between the walls of the packed bed and the spherical particles is also 2 mm.

Figure 4.1 gives the schematic diagram of the system under study. Entry length of 140 mm is provided so that velocity profile is nearly fully developed. Similarly a distance of 120 mm is provided after the top layer of the spherical particles.

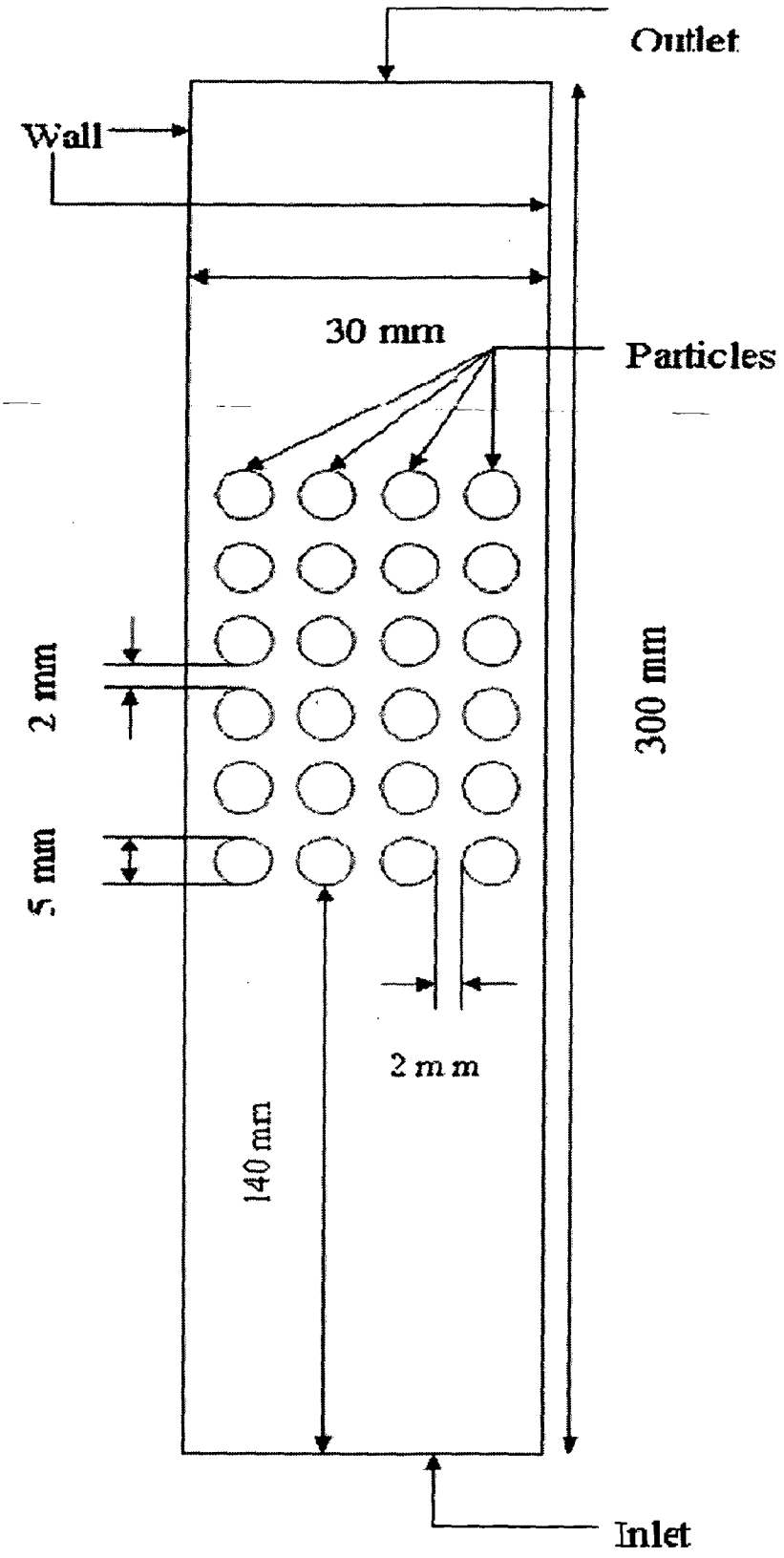

Fig.4.1 Schematic diagram of the system

METHODOLOGY

The commercial package CFD code FLUENT 6.2.16 is used to simulate the model equations. Simulations are performed on Intel(R), Pentium(R) 4 CPU 2.66GHz, 512 MB of RAM based personal computer.

5.1 DEVELOPMENT OF GEOMETRIC MODEL

Geometrical model (or physical model) has been developed using GAMBIT 2.2.30 as follows. The packed of spheres is modeled with dimensions 300 mm length and 30 mm diameter. Particles of diameter 5 mm are at 140 mm from the inlet. There are six layers of spherical particles and each layer is consists of four spherical particles thus there are total 24 spherical particles considered in the present model.

5.2 BOUNDARY CONDITIONS AND FLOW PROPERTIES

Boundary conditions used for the flow variables in the simulation as listed in table 5.1

Table 5.1: Boundary conditions for the flow variables

Variable	Wall	Inlet	Outlet
u	0	0	outflow
v	0	0.1 m/s at X=0m, Y=2.755m to Y=3.505m, Z=2.5m to Z=3.25m	outflow
w	0	0	outflow
k	k-equation	TI=5%,L=0.01 m	zero gradient
e	wall-function	TI=5%,L=0.01 m	zero gradient

In numerical simulations, fluid properties are held constant with value corresponding to a operating temperature of 25^0C. The water density is 1000 kg/m^3, viscosity is $1.003*10^{-3}$ kg/(ms), specific heat is 4182 J/(kg-K) and Thermal conductivity is 0.6 W/(mK).

The fluid properties are summarized in the Table 5.2

Table 5.2: fluid properties

Fluid	**Density kg/m^3**	**Viscosity kg/(ms)**	**Specific heat J/(kgK)**	**Thermal conductivity w/(mk)**
Water	1000	1.003e-03	4182	0.6

5.2.1 INLET CONDITION:

Uniform distribution is used over the inlet boundary of the vertical velocity, u_o. Other quantities such as pressure and the other two velocity components are taken as zero at the inlet.

The kinetic energy of turbulence is calculated using

$$k= (3/2)\, I^2 u_o^2 \qquad (56)$$

Where I^2 is the turbulence intensity of the u-component of velocity at the inlet which is taken as 0.14 in the absence of measured values,

The dissipation rate is obtained from

$$\varepsilon= k^{1.5}/ (\lambda H) \qquad (57)$$

5.2.2 OUTLET CONDITIONS:

The vertical component of velocity u_e is derived from the continuity equation, i.e.

$$u_e = u_o \frac{A_o}{A_e}\frac{\rho_o}{\rho_e} \qquad (58)$$

and the other velocity components and the pressure are assumed to be zero. Boundary conditions for k and ε are not required because an up-wind computational scheme, is used expect that their gradients in the exit plane are zero. Uniform distribution of u_e and T_e is assumed across the exit area.

5.2.3 WALL BOUNDARY:

Close to a wall region laminar viscosity becomes more significant than turbulent viscosity as a result of the damping effect of the wall, i.e. $\frac{\partial}{\partial y}(k)=0$ at the wall. So the turbulence model equations do not apply to regions close to a solid boundary and instead the wall-function equations due to launder and spalding are used for the velocity component parallel to the boundary. With in the laminar sublayer region viscous effects pre-dominate and the wall shear stress, τ_w, is described by the usual couette flow expression. At a point outside this region turbulent shear becomes significant and it can be shown that when the generation and dissipation of energy is in balance then $\frac{\tau}{\rho}=C_\mu{}^{0.5}k$

5.3 NUMERICAL SOLUTION PROCEDURE

In FLUENT, the continuous governing equations are converted into finite difference equations via integration over control volumes created by a uniform rectangular grid of 300×30 size. The second order upwind scheme is used to discretize the flow terms in space. Formally, this scheme exhibits first-order accuracy when the cell Reynolds number is low and second-order accuracy when the cell Reynolds number is high.

The discrete equations are solved under the imposed boundary conditions with an iterative procedure that implements the Line Gauss–Seidel method and the SIMPLE (semi-implicit method for pressure –linked equations) algorithm.

At inlet, water velocity is 7.312 mm/s with Re=519. The difficulty with this velocity is that the inlet contains a disturbed laminar flow. The inlet section is not long enough for the boundary layers to converge, so the majority of the inlet air velocity profile is that of laminar plug flow. The low flow velocity makes the system inherently more sensitive to small disturbances in the numerical simulation.

5.4 DEVELOPMENT OF GEOMETRIC MODEL ON GAMBIT

Accessing GAMBIT 2.2.30

Enter the GAMBIT environment then start creating geometry of the system.

Create Geometry in GAMBIT

5.4.1.1 Select Solver:

Specify that the mesh to be created is for use with FLUENT 6.0:

Main Menu > Solver > FLUENT 5/6

The boundary types depend on the solver selected.

5.4.1.2 Create Vertices:

Using vertex command create vertices.

Next to x: enter value 0. Next to y: enter value 0. Next to z: enter value 0 (these values should be defaults). Click Apply. This creates the vertex (0,0,0) which is displayed in the graphics window

In the *Transcript* window, GAMBIT reports that it "Created vertex: vertex.1". The vertices are numbered vertex.1, vertex.2 etc. in the order in which they are created.

This process is repeated to create three more vertices:

Vertex 2: (30,0,0)
Vertex 3: (30,300,0)
Vertex 4: (0,300,0)

For a 2D problem, the z-coordinate is always left to the default value of 0.

5.4.1.3 Create Edges:

Now appropriate pairs of vertices are connect to form edges. To select any entity in GAMBIT, hold down the Shift key and click on the entity.

Two vertices that make up an edge of this rectangle are selected by holding down the Shift button and clicking on the corresponding vertices. As each vertex is picked, it will appear red in the *Graphics Window*.

After the correct vertices have been selected, first click Close and then click Apply in the *Create Straight Edge* window and it creates an edge.

This process is repeated to create a rectangle.

5.4.1.4 Create Face:

To form a face out of the area enclosed by the four lines, we need to select the four edges that enclose this area. This can be done by holding down the Shift key, clicking on each line (notice that the currently selected line appears red), and then releasing the Shift key after all four lines have been selected.

Click Close followed by apply button and the face is created.

5.4.1.5 Create Circular Faces:

Circular face option is selected through operation tool pad.

Next value of Radius is to be entered. Enter the value (2.5) Apply and Close buttons are selected to create the circular face. It is created at the origin. Now using Move / Copy / Align Faces button, this will bring up the Move / Copy panel and selecting the circular face value of X (4.5) and Y(140) are entered. It moves the selected face to the desired position.

Whole process is repeated to create another five circular faces and move and align them at desired location.

5.4.1.6 Subtract the Faces:

Select face.1 next to Face and face.2 next to Subtract Faces from Subtract Faces panel and the press Apply and then Close.

Repeat this process to subtract the other circular faces from the face.1.

5.4.2 Mesh Geometry:

Now a mesh is to be created on the rectangular face with 400 divisions in the vertical direction and 50 divisions in the horizontal direction. First the four edges are meshed and then the face. The desired grid spacing is specified through the edge mesh.

5.4.2.1 Mesh Edges:

The *Edge List* window is brought up and both the vertical lines are selected. To return to the main view, click on the Global Control Toolpad > Fit to Window Button again.

Once a vertical edge has been selected, Interval Count is selected from the drop down box that says Interval Size in the *Mesh Edges Window*

Click Apply. Nodes appear on the edges showing that they are divided into 400.

The same process is repeat for the horizontal edges, but with an interval count of 50.

5.4.2.2 Mesh Face:

Shift left-click on the face or the up arrow next to Faces is used to select the face and then click Apply.

5.4.3 Specify Boundary Types:

5.4.3.1 Create Boundary Types:

Next the boundary types in GAMBIT are set. The bottom edge is the inlet of the pipe, the top edge the outlet and the left and right edges the wall.

First the bottom edge is selected by Shift-clicking on it. The selected edge would appear in the yellow box next to the Edges box.

Next to Name: enter inlet.

For Type: select VELOCITY_INLET.

Click Apply.

This process is repeated for the other three edges according to the following table 5.3

Table 5.3

Edge Position	Name	Type
Bottom	inlet	VELOCITY_INLET
Top	outlet	PRESSURE_OUTLET
Left	wall	WALL
Right	wall	WALL

5.4.4 Save and Export:

First file is saved and then exported using a file name (packedbed.msh) for the File Name: Select Export 2d Mesh since this is a 2 dimensional mesh. Click Accept.

Check packedbed.msh has been created in working directory.

The geometry created is shown in the Fig.5.1

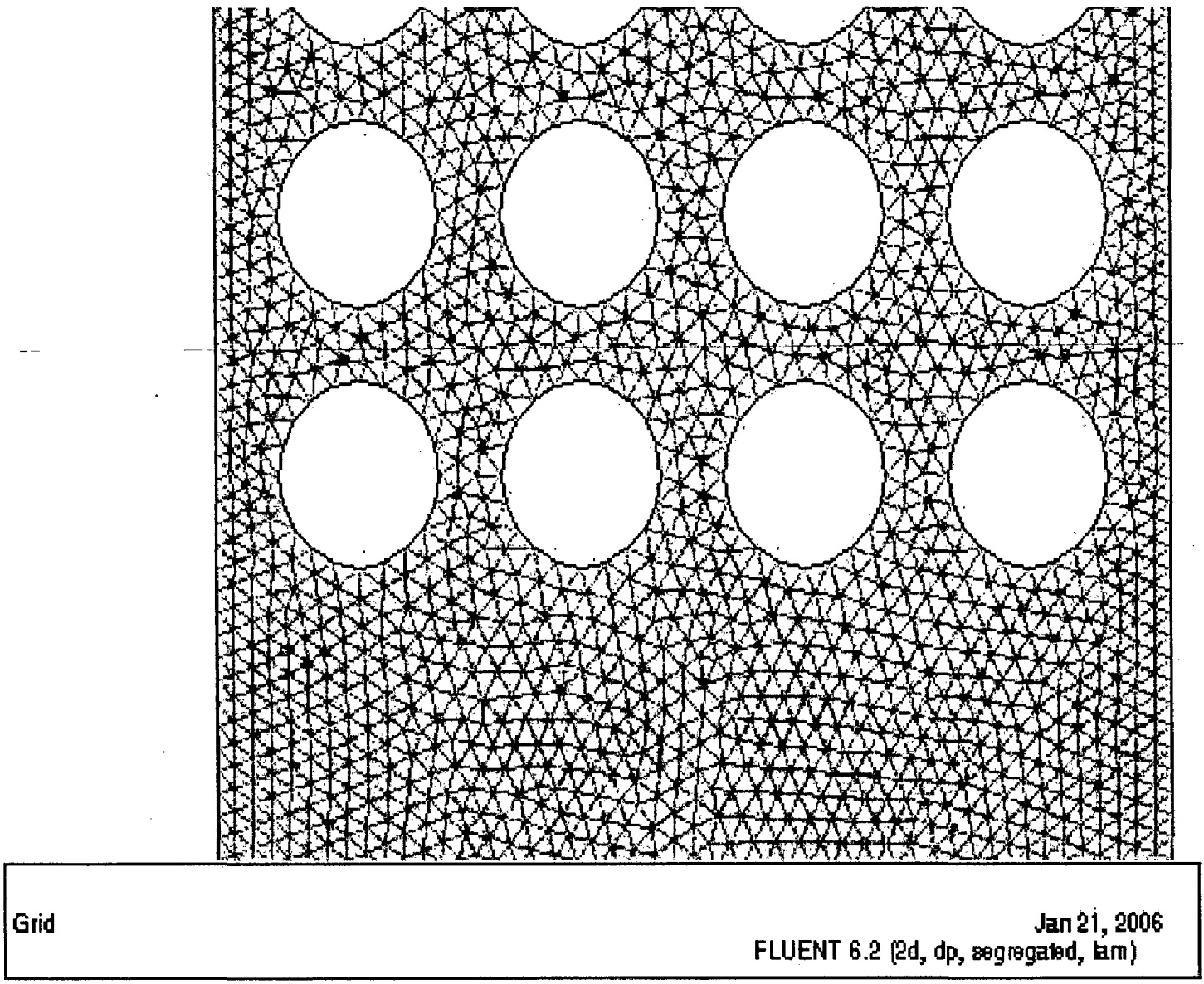

Fig.5.1 Grid generated in Gambit

RESULTS AND DISCUSSION

6.1 GENERAL

System of spherical particles in a tube described in chapter 4 is simulated and solved for two dimensional model using boundary conditions given in chapter 5. steady state solutions are obtained using CFD code FLUENT 6.2.16 on a PC having Pentium IV CPU.

6.2 SOLUTION INITIALIZATION AND ITERATION

Solution initialization and iteration are carried out till the solution gets converged on convergence criteria 0.0001. Two different representation of the fluid flow in the packed bed are used: laminar flow, turbulent flow using the standard k-ε turbulence model. The governing equations for the packed bed system are the mass conservation equation and the Navier-Stokes equations.

For laminar simulation:-

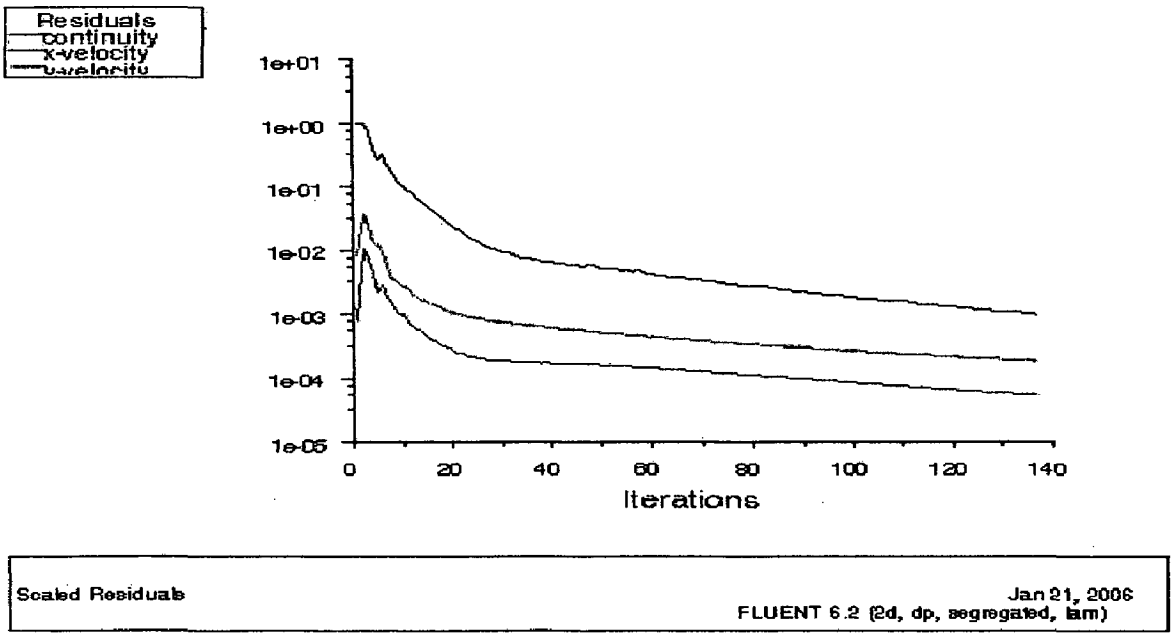

Fig.6.1 Convergence for laminar model

From fig.6.1, for laminar model number of iterations for convergence is 137 and time taken for convergence is 15 minute 39 second.

For standard k-ε simulation:-

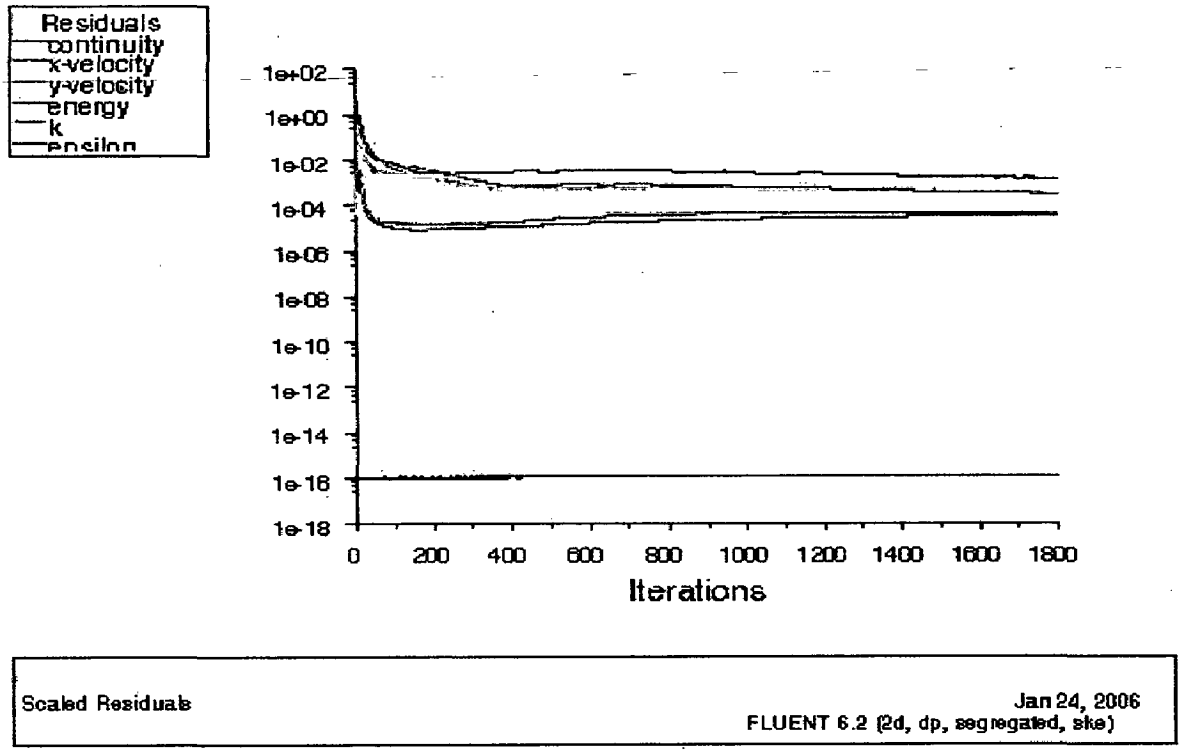

Fig.6.2 Convergence for k-ε model

From fig.6.2, for k-ε model, it is clear that more iterations are required. The number of iterations for convergence is 1792 that is much more than laminar model with simulation time 35 minute 57 second.

Therefore k-ε model is more time consuming than laminar model and the rate of iteration is also slow in comparison with laminar model. This is due to more number of equations used in k-ε model as compared to laminar model.

6.3 PROFILES OF DIFFERENT PARAMETERS

Vectors and contours of velocity of water and pressure distribution is important for the analysis of packed bed. For this purpose, data of different variables studied has been obtained at different distances from the inlet of the packed bed i.e. Y=0.015m, Y=0.025m, Y=0.100m, Y=0.136m, Y=0.1375m, Y=0.1435m, Y=0.1775m, Y=0.179m, Y=0.210m and Y=0.250m and plots are plotted.

6.3.1 Variation/Profiles of Velocity

In this present work simulations have been carried out to obtain the velocity profile in the packed bed for different inlet fluid velocities. For laminar model the velocities of 1.378 mm/s, 7.312 mm/s and 9.8 mm/s have been used with varying pressures in the range of 2 kPa – 150 kPa. For K-ε model the velocity of 20.548 m/s at atmospheric pressure has been used.

6.3.1.1 Velocity profiles for 1.38 mm/s at 2 kPa

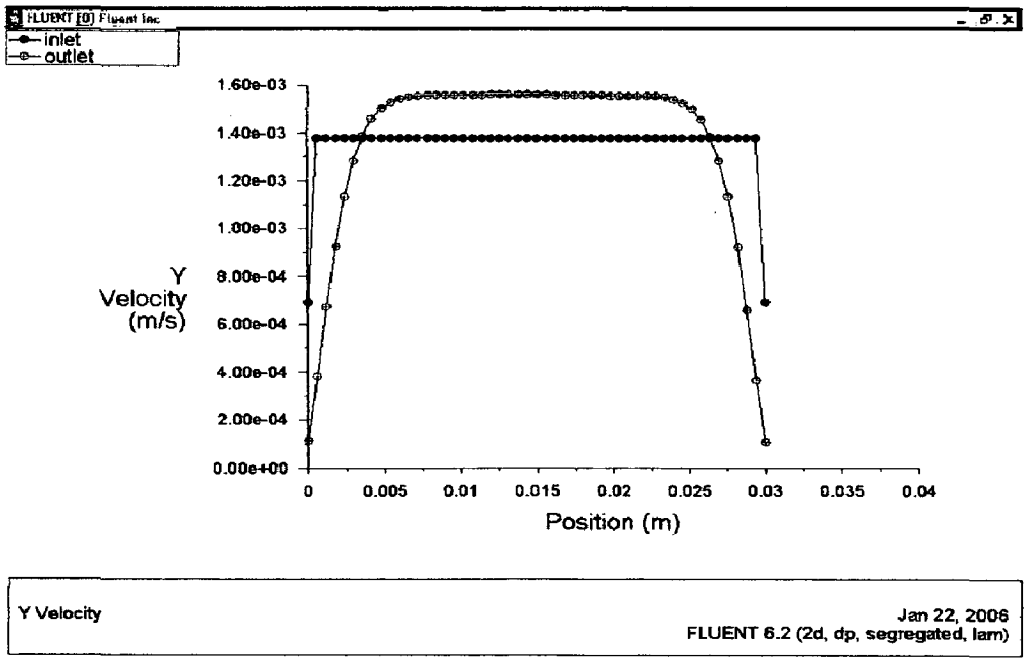

Fig.6.3 Velocity profile for 1.38 mm/s at inlet and outlet

From fig.6.3 it can be seen that velocity is high at the center of the packed bed. At the inlet the velocity is uniformly distributed and the value of the velocity is 1.38 mm/s. At the outlet the profile of the velocity distribution is nearly parabolic and the maximum value of the velocity at the outlet is approximately 1.57 mm/s. From fig.6.3 it can be seen that near the wall velocity is very low and it is increasing with respect to increase in distance from the wall to the center. Contour plot corresponding to this velocity profiles is in fig.6.4.

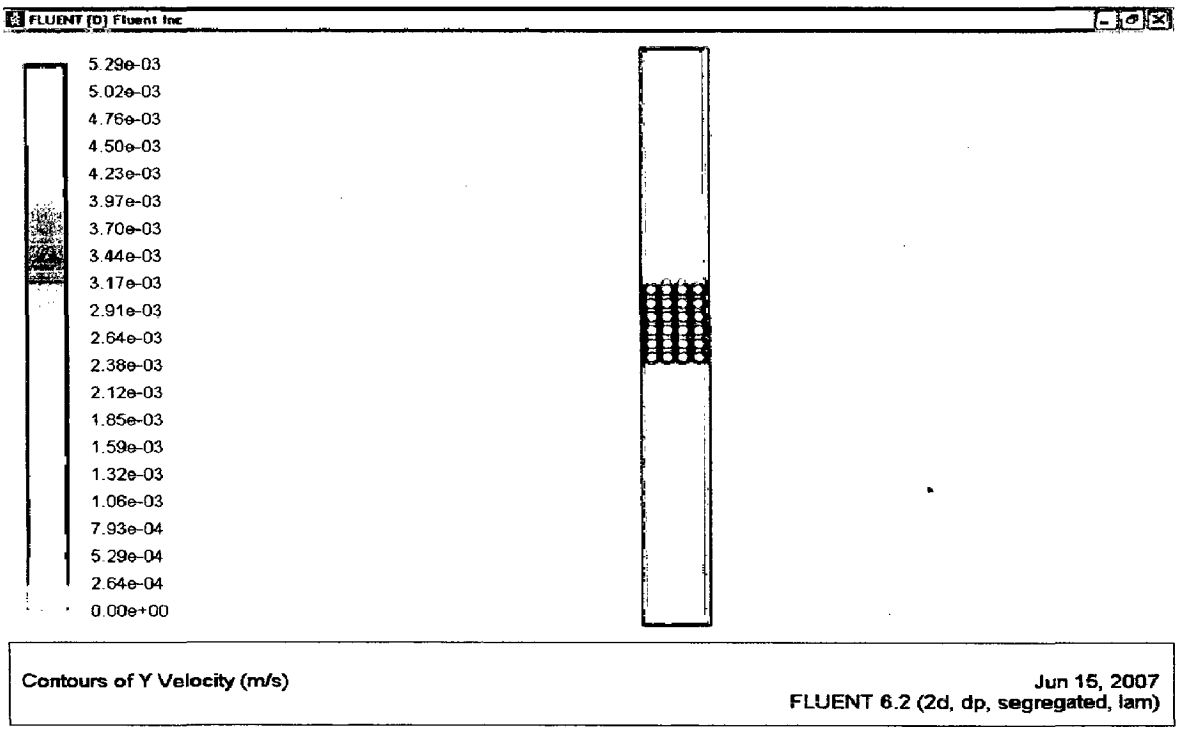

Fig.6.4 Contour plot of velocity at 1.38 mm/s

Fig.6.5 is a plot of velocity as a function of position across the column for different height along the column. In this fig it is seen that velocity profiles at 25 mm and 100 mm from inlet are similar and nearly parabolic and the value of velocity is 1.5 mm/s. Near the particles (136 mm) and at the surface of the particles (137.5 mm), it can be seen from the fig.6.5 that the oscillation pattern of velocity has a similar tendency. The velocity has a zero value at the column wall, reaching the first peak value at 2.5 mm from the wall and has a minimum at 5 mm. The velocity at first peak for Y=136 mm is about 1.75 mm/s and for Y=137.5

mm is about 2.5 mm/s, this value of velocity is between wall and the particle near the wall. The velocity continues cycling with interval distance of peaks about 5 mm. The value of velocity at second peak for Y=136 mm is about 1.85 mm/s and for Y=137.5 mm is about 3 mm/s. The velocity at second peak is the velocity between two adjacent particles. The velocity near the particles is low and velocity between two adjacent particles is higher, it is obvious because between two adjacent particles the available area for the flow is much less and from the equation of continuity the velocity will increase.

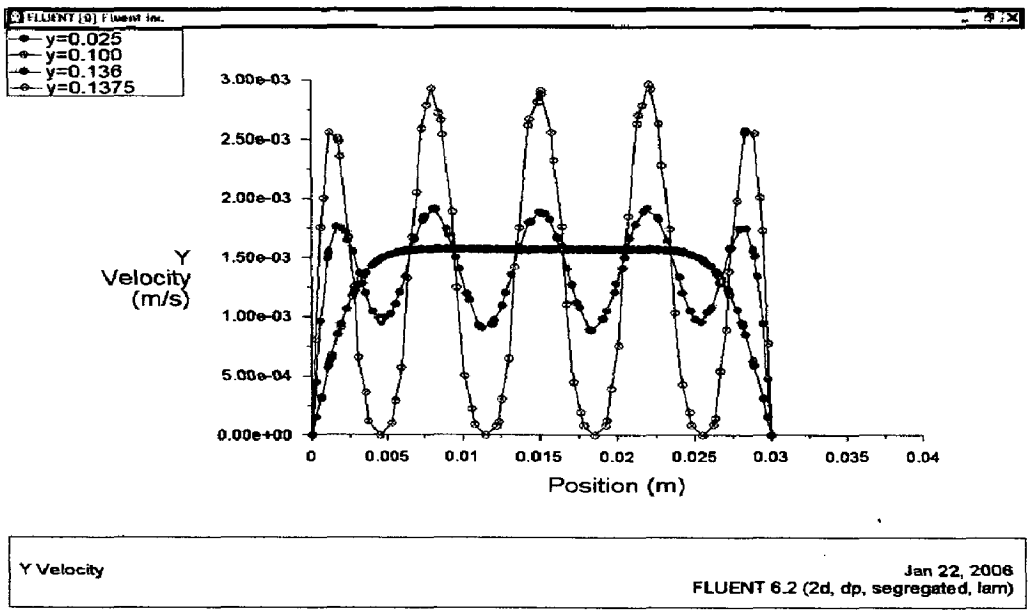

Fig.6.5 Velocity profile at 1.38 mm/s at different distances

Consequently, the behavior of velocity is jet like between the particles and the value is much high than the free stream velocity.

Further from the vertical distances along the length, the oscillation pattern of velocity continues between the particles. It is evident from the fig.6.6, that the velocity at first peak for Y=143.5 mm and for Y=177.5 mm is same and the value is 2.75 mm/s.

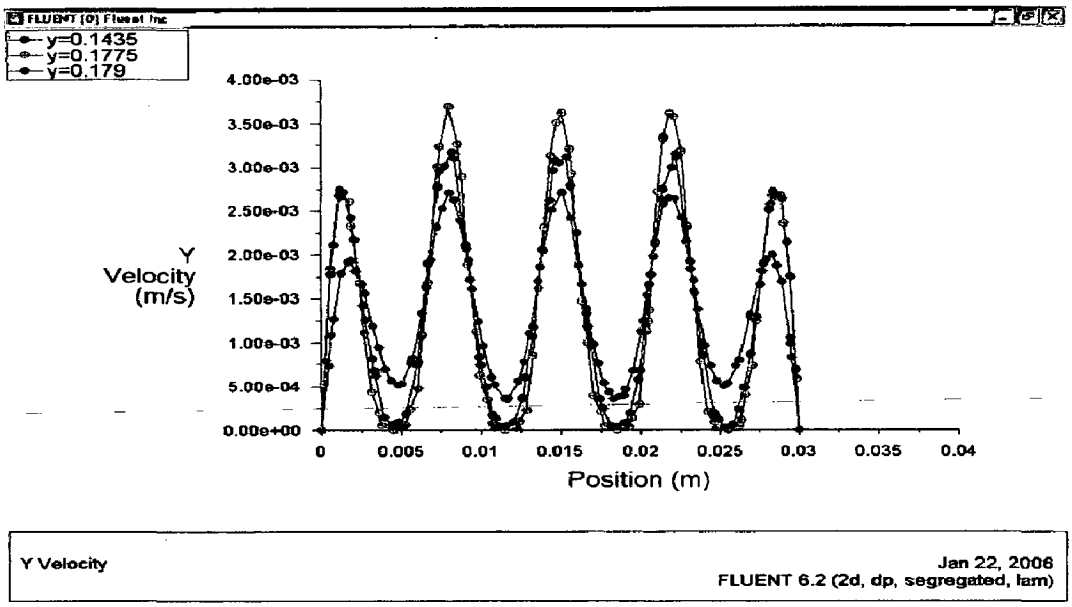

Fig.6.6 Velocity profile at 1.38 mm/s at different distances between particles

The velocity away from the particles and to the outlet begins to decrease but the oscillating behavior is maintained for some distance. This can be seen from Fig.6.6 that the velocity for Y=179 mm is about 2.75 mm/s.

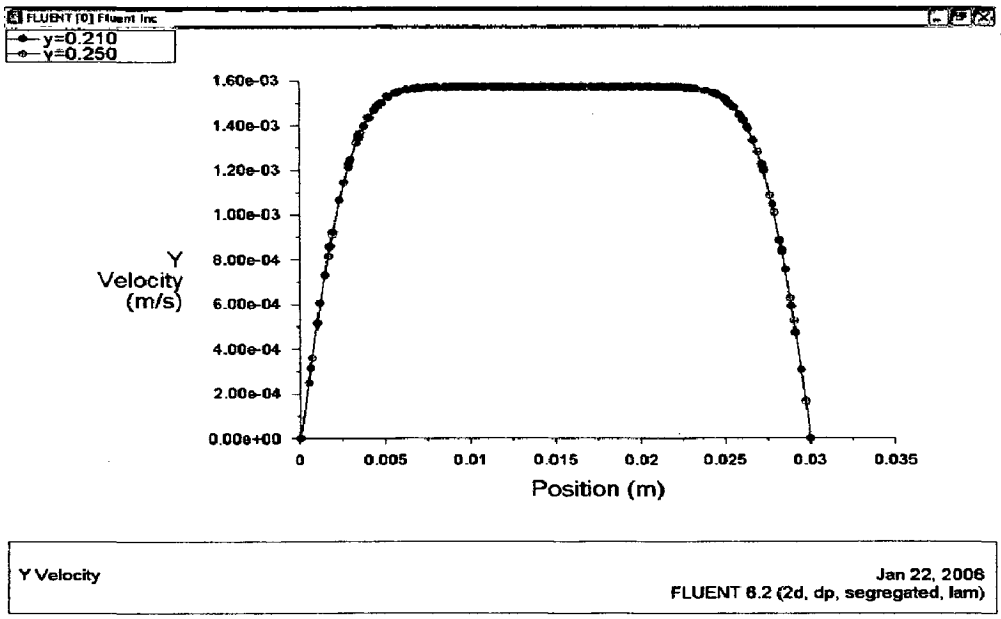

Fig.6.7 Velocity profile at 1.38 mm/s at different distances away from particles

After some distance this behavior diminishes. It is evident from Fig. 6.7 that for Y=210 mm and Y=250 mm the oscillating behavior disappears and distribution is

same for both the cases. The velocity for both the cases is found to be about 1.58 mm/s.

6.3.1.2 Velocity profiles for 7.312 mm/s at 101.325 kPa

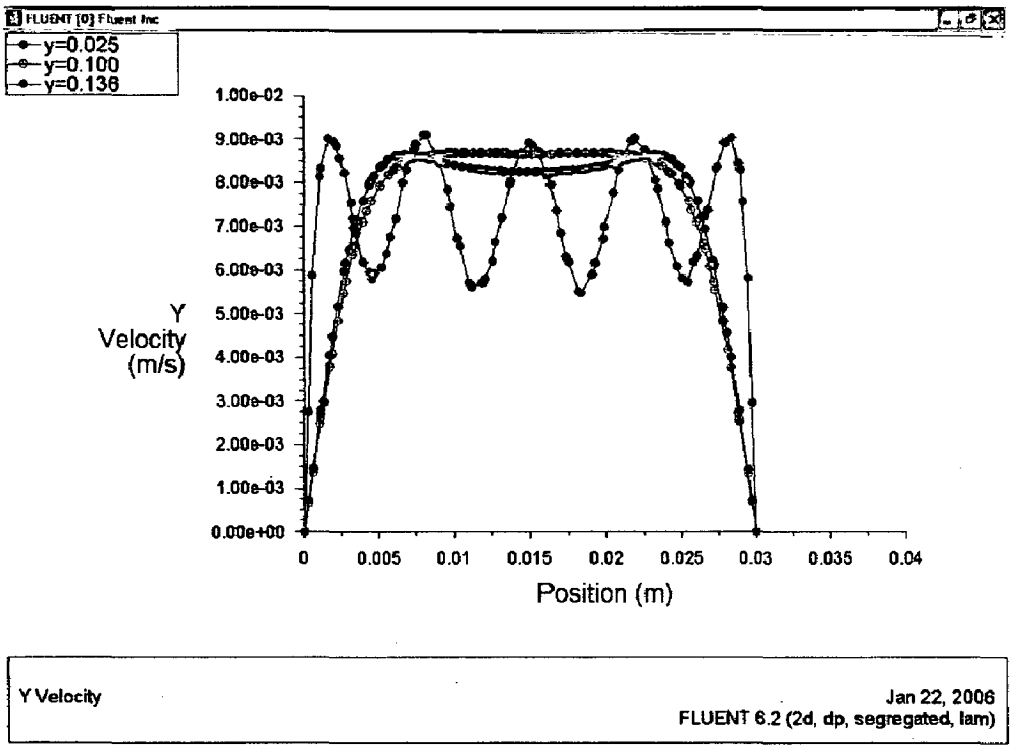

Fig.6.8 Velocity profile at 7.312 mm/s at different distances from inlet

From fig.6.8 velocity profiles for Y= 25 mm and for Y=100 mm from inlet are not similar. For Y=100 mm the profile is nearly parabolic and the value of velocity is 8.9 mm/s. Near the particles for Y=136 mm, it can be seen from the fig.6.8 that the oscillation pattern of velocity has a similar tendency. The velocity has a zero value at the column wall, reaching the first peak value at 2.5 mm from the wall and has a minimum at 5 mm. The velocity at first peak for Y=136 mm is about 9 mm/s, this value of velocity is between wall and the particle near the wall. The velocity continues cycling with interval distance of peaks about 5 mm. The value of velocity at second peak for Y=136 mm is similar. The velocity at second peak is the velocity between two adjacent particles.

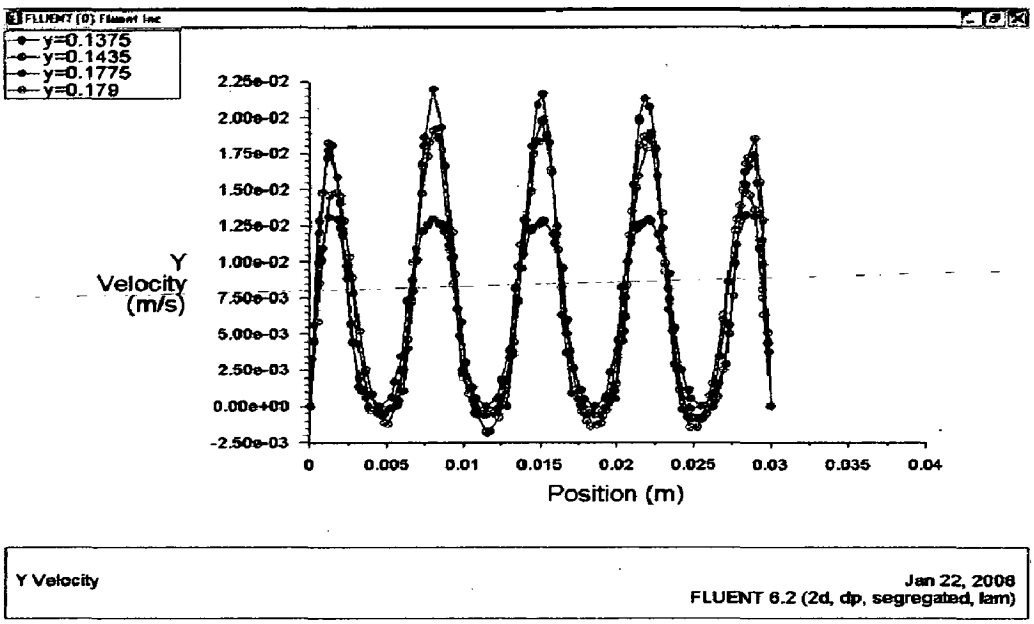

Fig.6.9 Velocity profile at 7.312 mm/s at different distances between particles

Further from the vertical distances along the length, the oscillation pattern of velocity continues between the particles. It is evident from the fig.6.9, that the velocity at first peak for Y=137.5 mm, Y=143.5 mm, Y=177.5 mm and for Y=179 mm are oscillating and the value are 1.3 mm/s, 1.85 mm/s, 1.75 mm/s and 1.46 mm/s respectably. It is clear from the plot that for Y=179 mm the oscillating behavior does not disappear as the case in the 1.38 mm/s velocity profile.

From fig.6.10, it is clear that the oscillating behavior is disappear further distances away from particles. At Y=210 mm the velocity profile is not parabolic but trying to be parabolic and the centerline velocity at this distance is about 10 mm/s. But at Y=250 mm the velocity profile is nearly parabolic and the centerline velocity in this case is found to be about 8.75 mm/s.

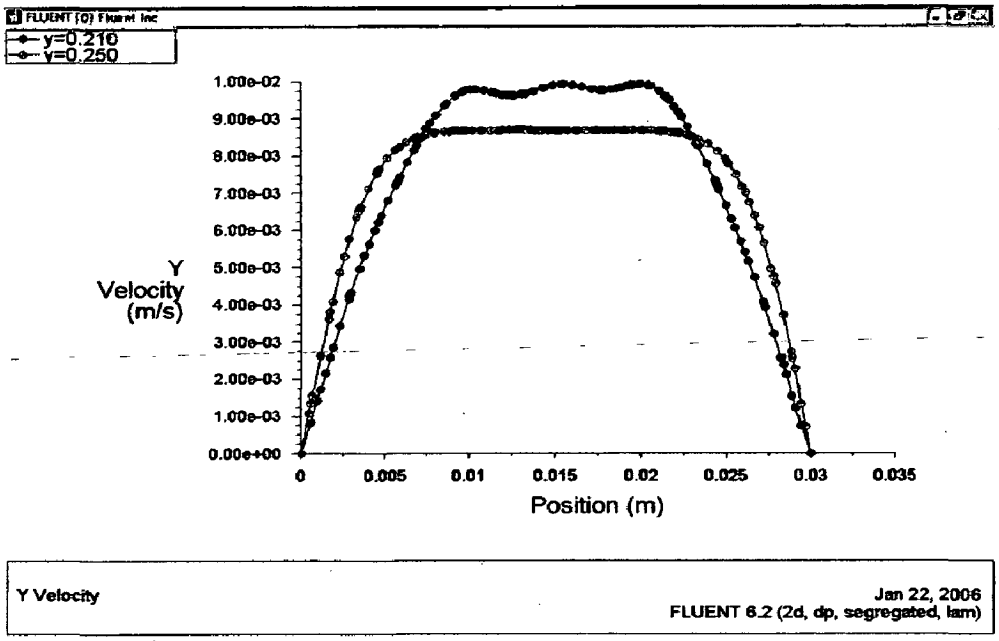

Fig.6.10 Velocity profile at 7.312 mm/s at different distances away from particles

The contour plot corresponding to the velocity of 7.312 mm/s is shown in Fig.6.11 and it provides the god qualitative representation of the discussion made using Fig.6.8 through Fig.6.10.

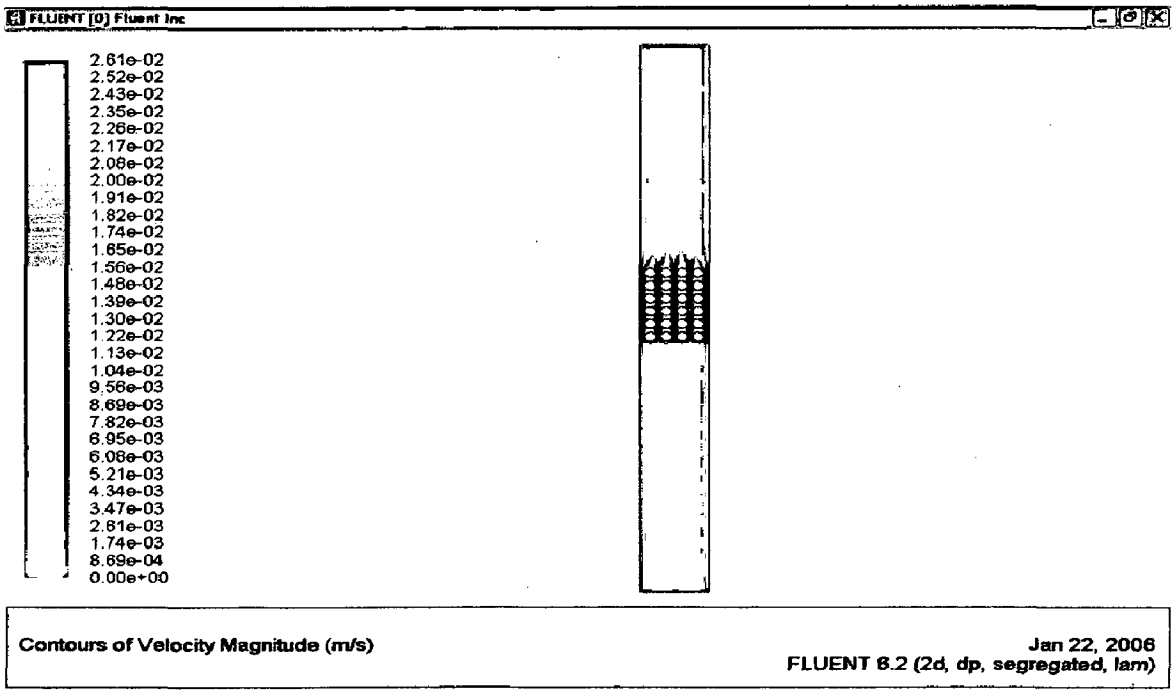

Fig.6.11 Contour plot of velocity at 7.312 mm/s

6.3.1.3 Velocity profiles for 9.8 mm/s at 150 kPa

The contour plot corresponding to the velocity of 9.8 mm/s is shown in Fig.6.12.

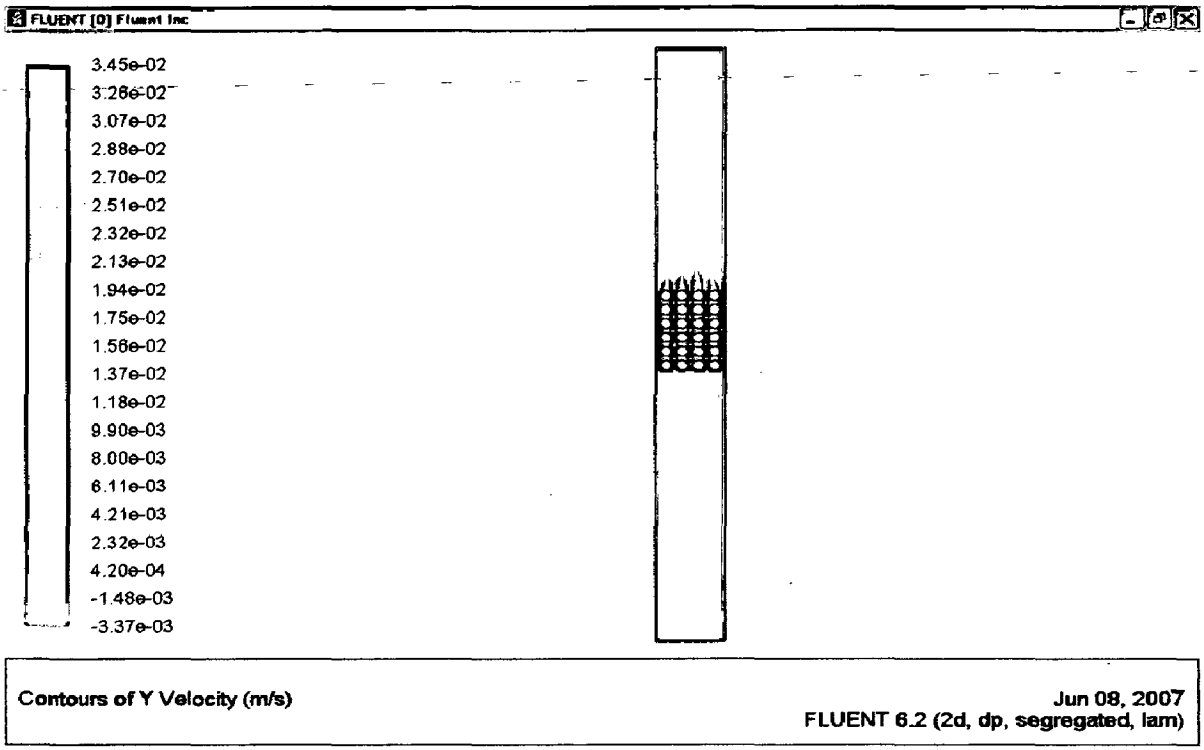

Fig.6.12 Contour plot for velocity of 9.8 mm/s

From Fig.6.12, it is clearly evident that the variations in velocity are more significant than the variations at lower velocities discussed earlier in this chapter. Further plots at different values of Y has been made and given in Figures 6.13 to 6.18.

From Fig.6.13, it can be easily seen that the velocity distribution is uniform at the inlet of the packed bed and at the outlet of the bed, the distribution of the velocity is exactly parabolic in nature at the outlet of the bed, which is not achieved at other inlet velocities. The average value of the velocity at the inlet is 9.8 mm/s

and the highest value of velocities at the outlet is found to be slightly higher than 14 mm/s.

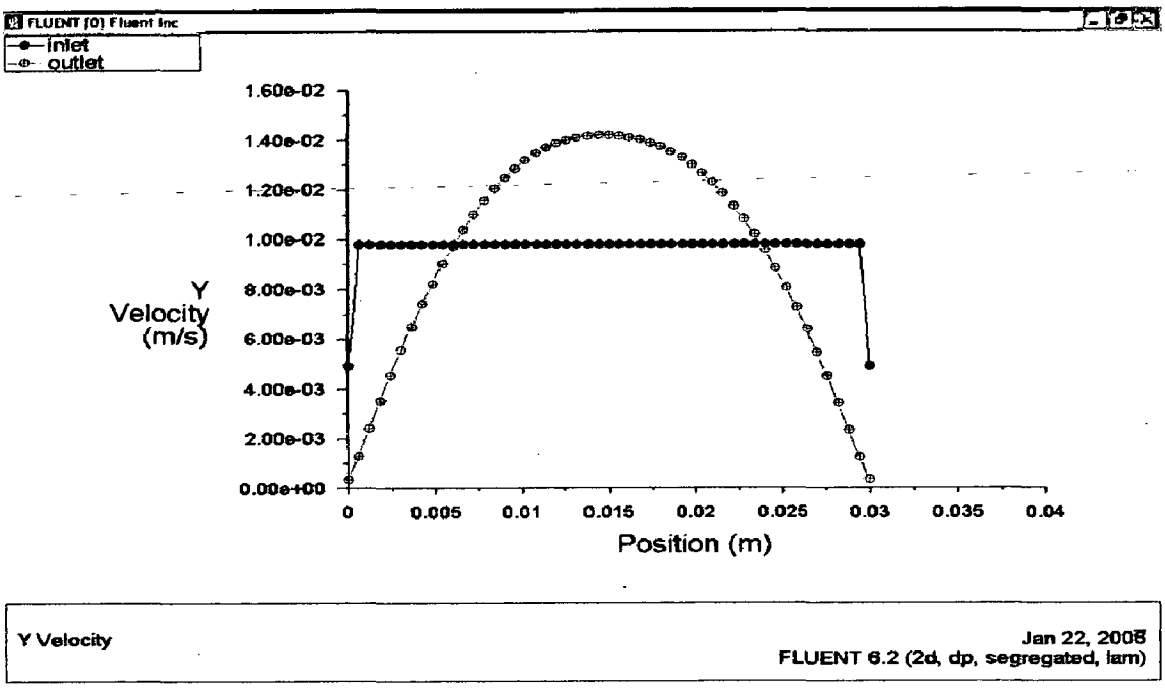

Fig.6.13 Velocity profile for 9.8 mm/s at inlet and outlet

The velocity profiles away from the inlet are shown in the Fig.6.14. It can be seen from the Fig.6.14 that at near the inlet at Y=25 mm, the profile is some what

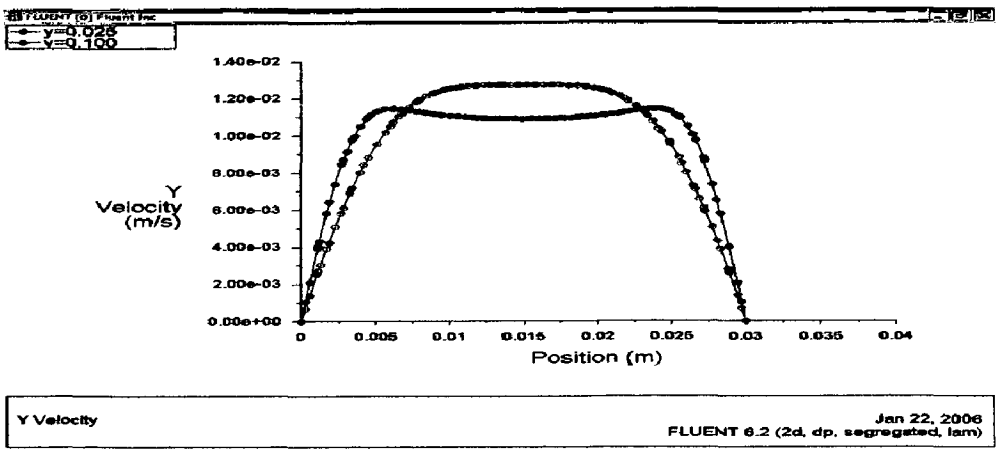

Fig.6.14 Velocity profile for 9.8 mm/s at different distances from inlet

deviates from the parabolic nature but trying to be parabolic in nature. But at a significant distance from the inlet i.e. Y=100 mm the distribution is nearly parabolic in nature. The value of the centerline velocity at Y=25 mm is found to be about 11 mm/s whereas the velocity at Y=100 mm this value is found to be around 12.8 mm/s, which is higher than the velocity at Y=25 mm.

From Fig.6.15, it can be easily seen that near the particles boundary the oscillating behavior of the velocity profile is again found.

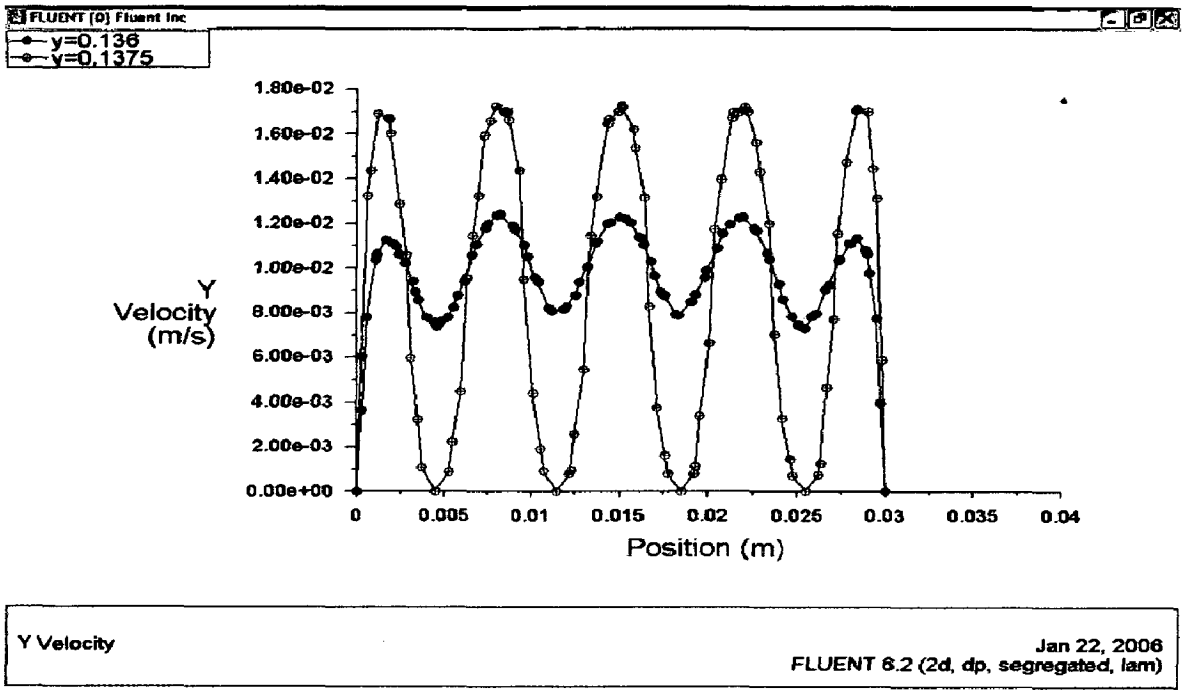

Fig.6.15 Velocity profile for 9.8 mm/s at different distances near particles

The velocity has a zero value at the column wall, reaching the first peak value at 2.5 mm from the wall and has a minimum at 5 mm. The velocity at first peak for Y=136 mm is about 11 mm/s, this value of velocity is between wall and the particle near the wall. The velocity continues cycling with interval distance of peaks about 5 mm (same size as that of spherical particles). The value of velocity at second peak for Y=136 mm is found to be about 12 mm/s. The

velocity at second peak is the velocity between two adjacent particles. The velocity at first peak for Y=137.5 mm is about 17 mm/s and the value of velocity at second peak for Y=137.5 mm is found to be similar, around 17 mm/s. The increase in the velocity between the wall and the particles and between two adjacent particles is clearly visible in the velocity profile.

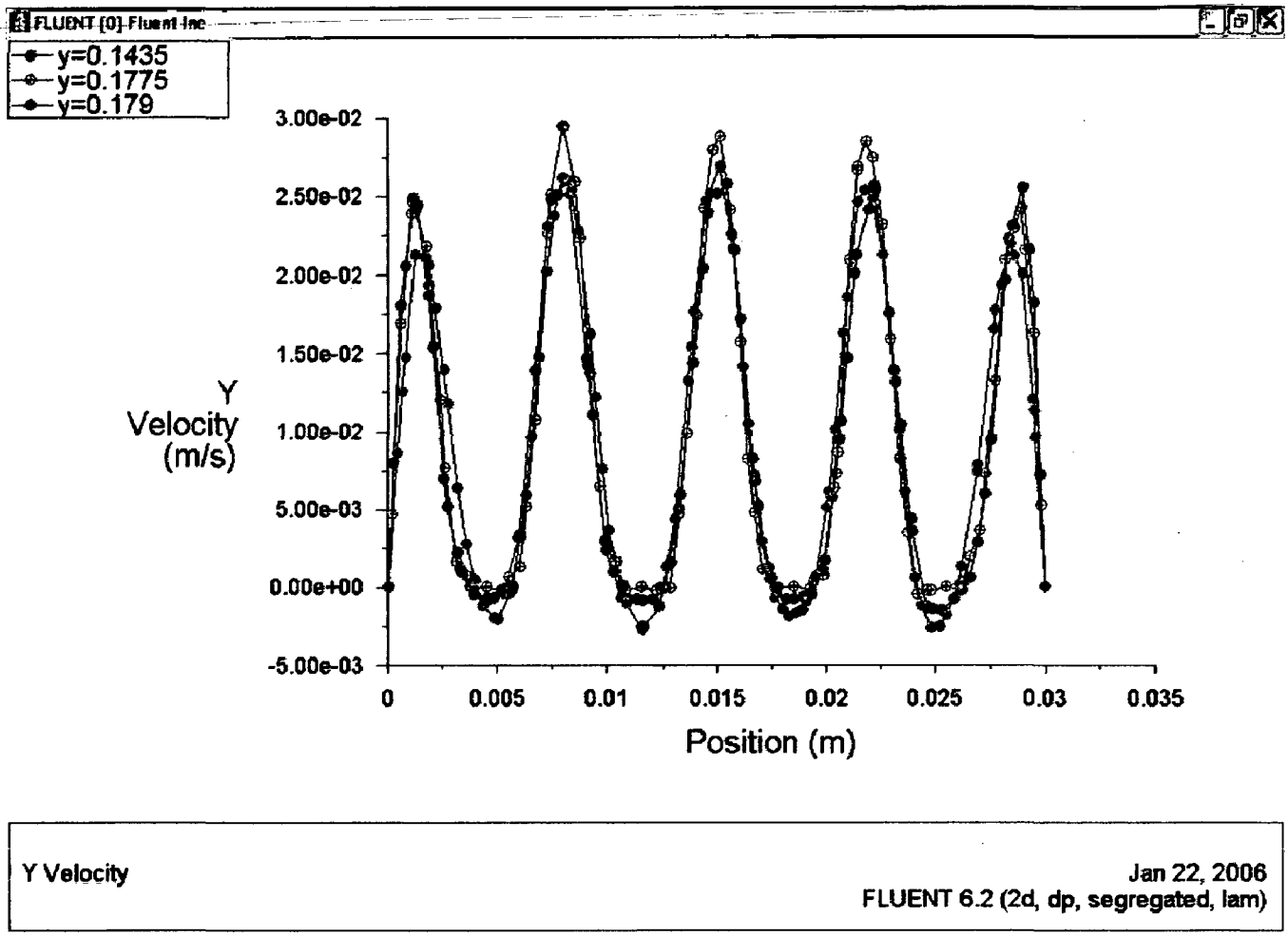

Fig.6.16 Velocity profile for 9.8 mm/s at different distances between particles

Between the particles the velocity profile is still found to be oscillating in nature at different distances. From Fig.6.16, it can be seen that the velocity profile at Y=1435 mm and at Y=177.5 mm the profile is very much similar and the value of velocity at first peak for Y=143.5 mm and Y=177.5 is about 25 mm/s, this value of velocity is between wall and the particle near the wall. The velocity continues

cycling with interval distance of peaks about 5 mm. The value of velocity at second peak for Y=143.5 mm is found to be about 26.5 mm/s and at Y=177.5 it is found to be around 29 mm/s. The velocity at second peak is the velocity between two adjacent particles. The value of velocity at first peak for Y=179 mm is about 22.5 mm/s and the velocity at second peak is nearly around 26.5 mm/s. The oscillating pattern in this case is also found.

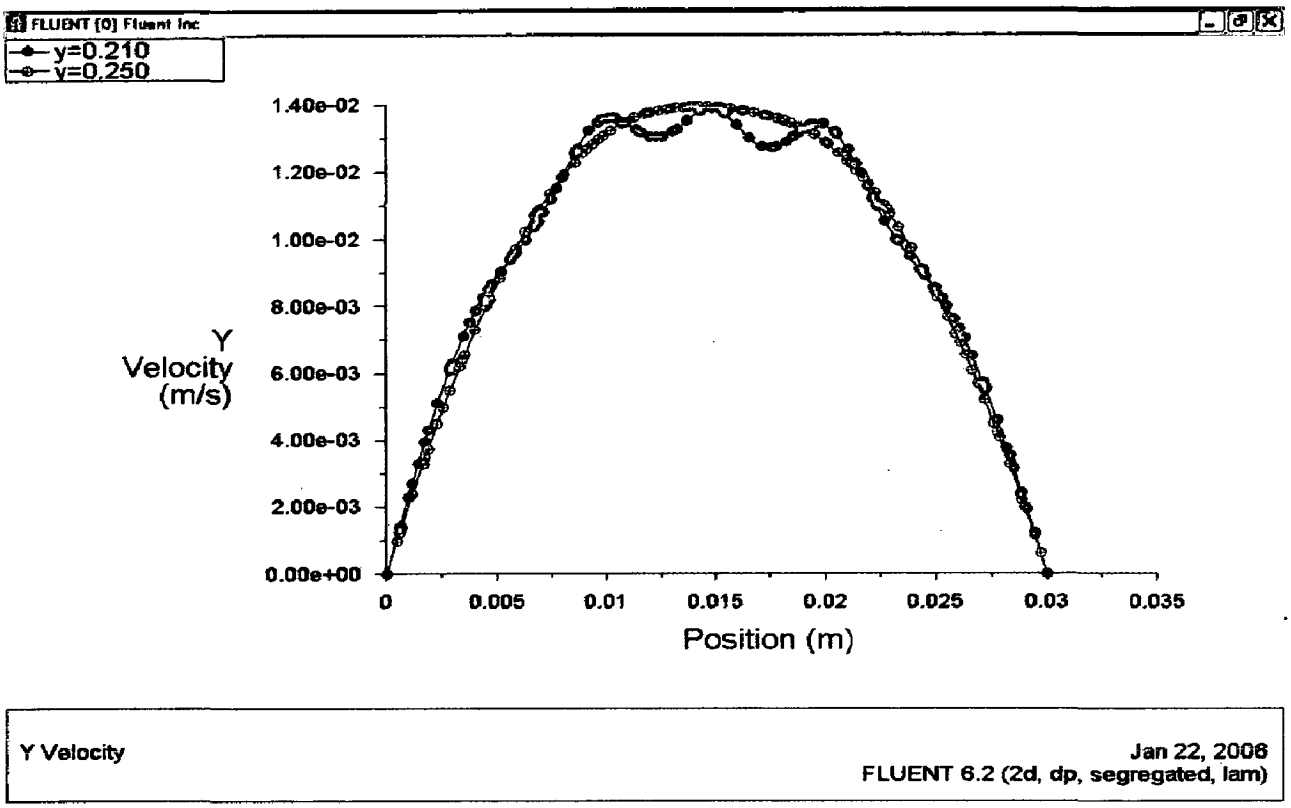

Fig.6.17 Velocity profile for 9.8 mm/s at different distances away from particles

As going away from the particles to the outlet of the packed bed, the oscillating pattern of velocity is not found and it disappears. It is evident from the Fig.6.17. It can be seen from this fig. that away from the particles to the outlet the pattern of the velocity is becoming parabolic. At Y=210 mm the velocity distribution is not exactly parabolic but it is tending to be parabolic. In this case the velocity at the centerline is still oscillating in nature but the oscillations are of low intensity the

minimum value of velocity at center is 12.4 mm/s and at the same time the maximum value of velocity at the center is found to be 13.8 mm/s. At Y=250 mm the velocity distribution is found to be parabolic with centerline velocity similar that of the maximum centerline velocity at Y=210 mm and the value of velocity is 13.8 mm/s.

At this velocity the eddies formation is also found between the two adjacent particles. But the eddies are of low intensity. The formation of eddies in this case is shown in the Fig.6.18.

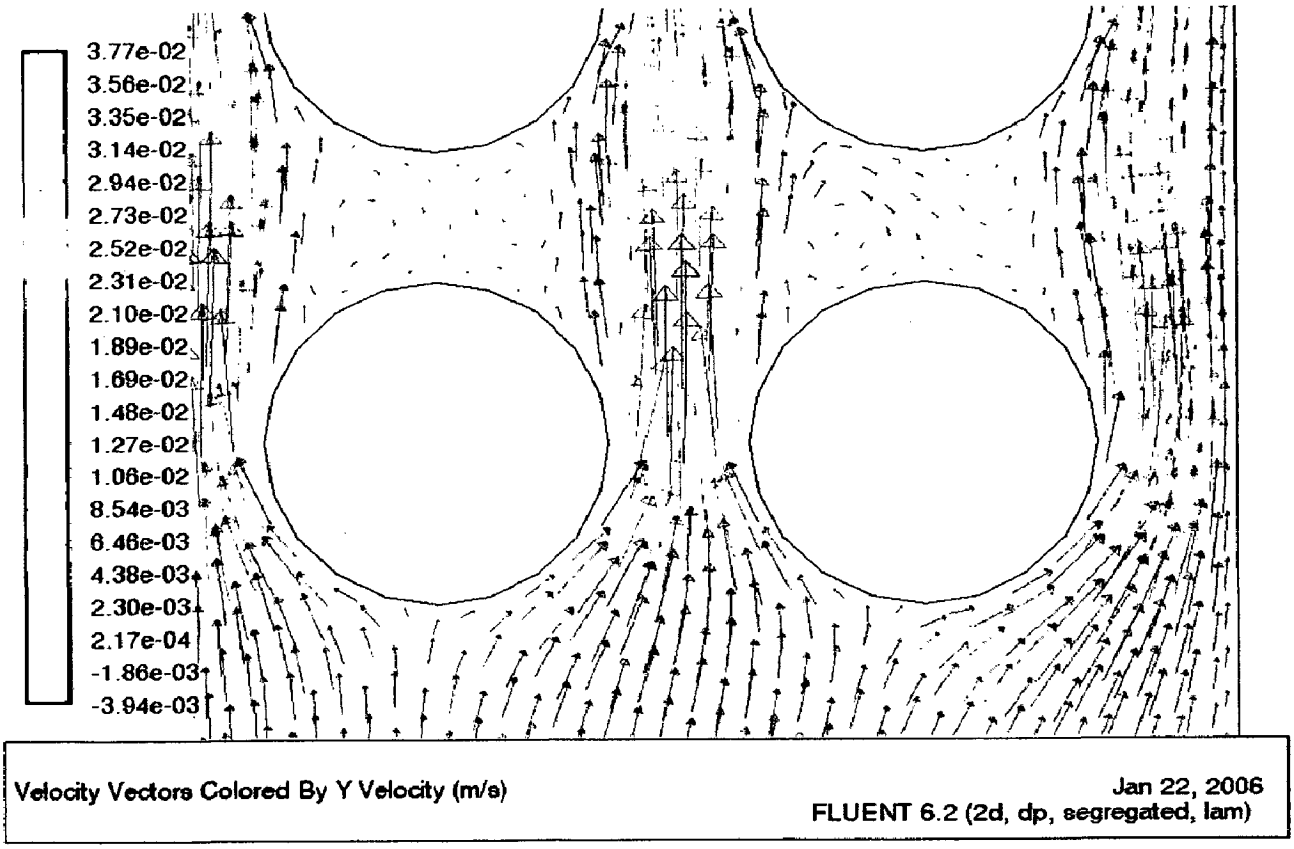

Fig.6.18 Eddies formation between two particles

From the velocity profiles in the packed bed it can be concluded that at the inlet some disturbance in the flow is found but after some distance from the inlet the parabolic distribution is attained. Near the particles the velocity profiles are found

to be of oscillating in nature due to the presence of the particles. Between the particles the jet like flow is observed because of the narrow area available for the flow. In between layers of particles eddy formation is observed. The oscillating pattern of velocity persists some distance after the particles and then becomes parabolic in nature near and at the outlet.

6.3.2 Variation/Profiles of Pressure

The variations of pressure at a given velocity is measured using simulations for different pressures. In this present work the pressure profile in the packed bed for different pressures of 2 kPa, 101.325 kPa and 150 kPa with varying velocities are used. For K-ε model the atmospheric pressure (101.325 kPa) has been used.

6.3.2.1 Pressure profiles at 2 kPa and at velocity of 1.378 mm/s

The contour plot for pressure distribution is shown in Fig.6.19.

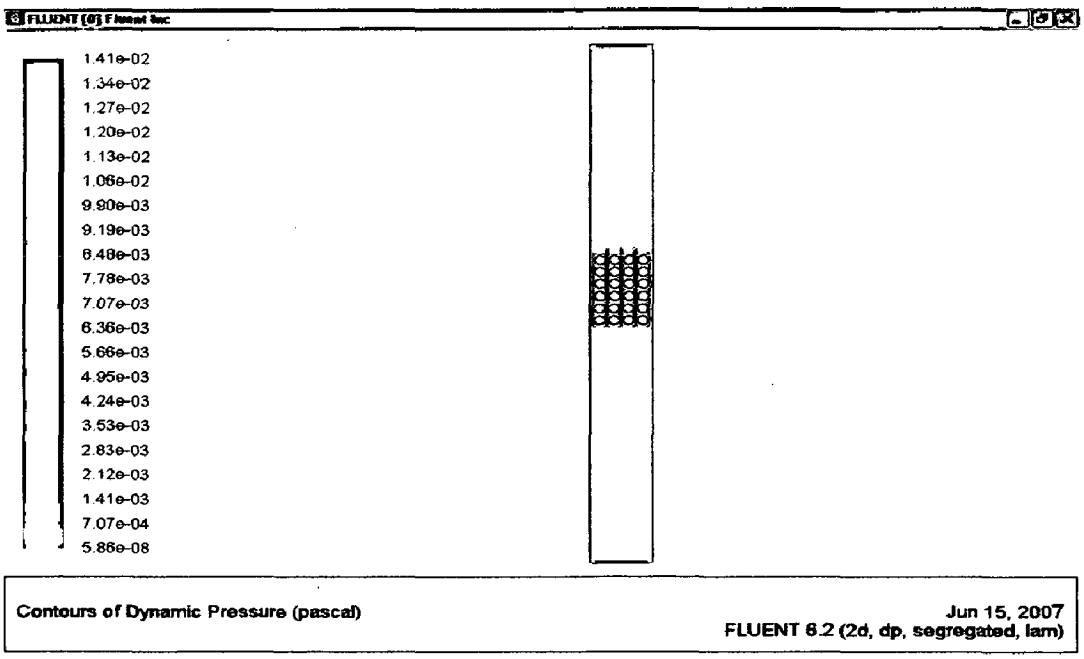

Fig.6.19 Contour plot for pressure at 2kPa

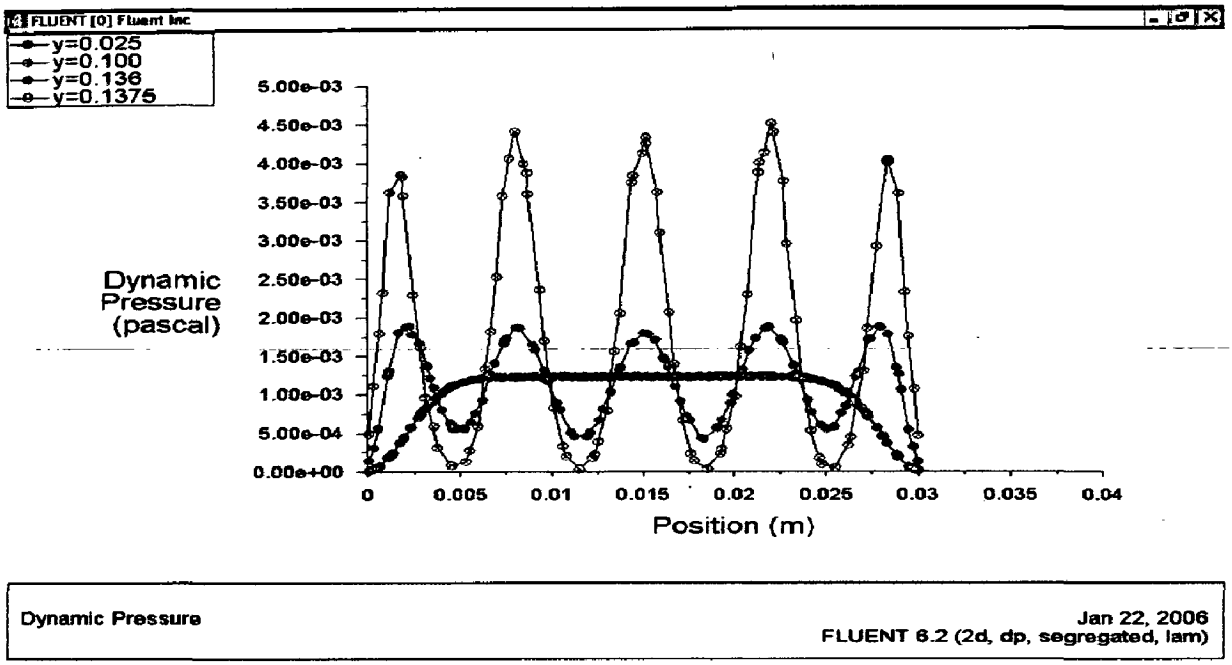

Fig.6.20 pressure profile for 2kPa at different distances near the particles

The dynamic pressure near the particles first increases and then it decreases throughout the diameter of the packed bed. The pressure increases between the wall and the adjacent particles and suddenly falls to the minimum value at the surface of the particle. The same nature of pressure is observed between the two adjacent particles. This phenomena is evident from the Fig.6.20, where the pressure profiles at Y=25 mm, Y=100 mm, Y=136 mm and Y=137.5 mm have shown. The pressure profiles at Y=25 mm and Y=100 mm are similar.

The similar nature of the pressure profiles have been found between the particles along the diameter of the packed bed. It can be seen from the Fig.6.21 where the pressure profiles at different distances along the length of the bed have been plotted. The same nature of the pressure profiles is observed as discussed above. Pressure increases between the wall and the adjacent particles and suddenly falls to the minimum value at the surface of the particle.

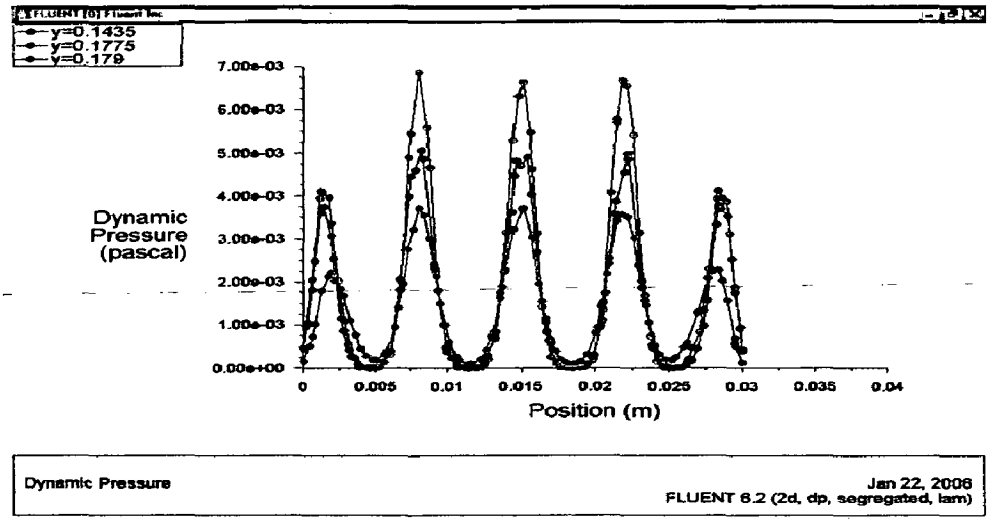

Fig.6.21 pressure profile for 2kPa at different distances between particles

The pressure profiles away from the particles are shown in the Fig.6.22. The pressure at Y=210 mm and Y=250 mm from the inlet have similar profiles. The pressure is lower at the wall and has the maximum value at the center of the packed bed. Both profiles coincide with each other.

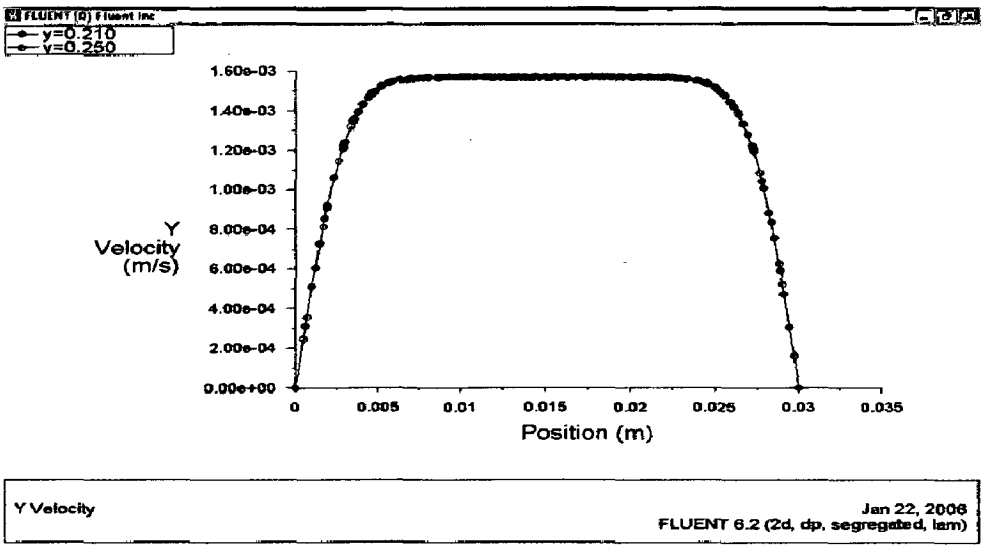

Fig.6.22 pressure profile for 2kPa at different distances away from particles

6.3.2.2 Pressure profiles at 101.325 kPa and at velocity of 7.312 mm/s

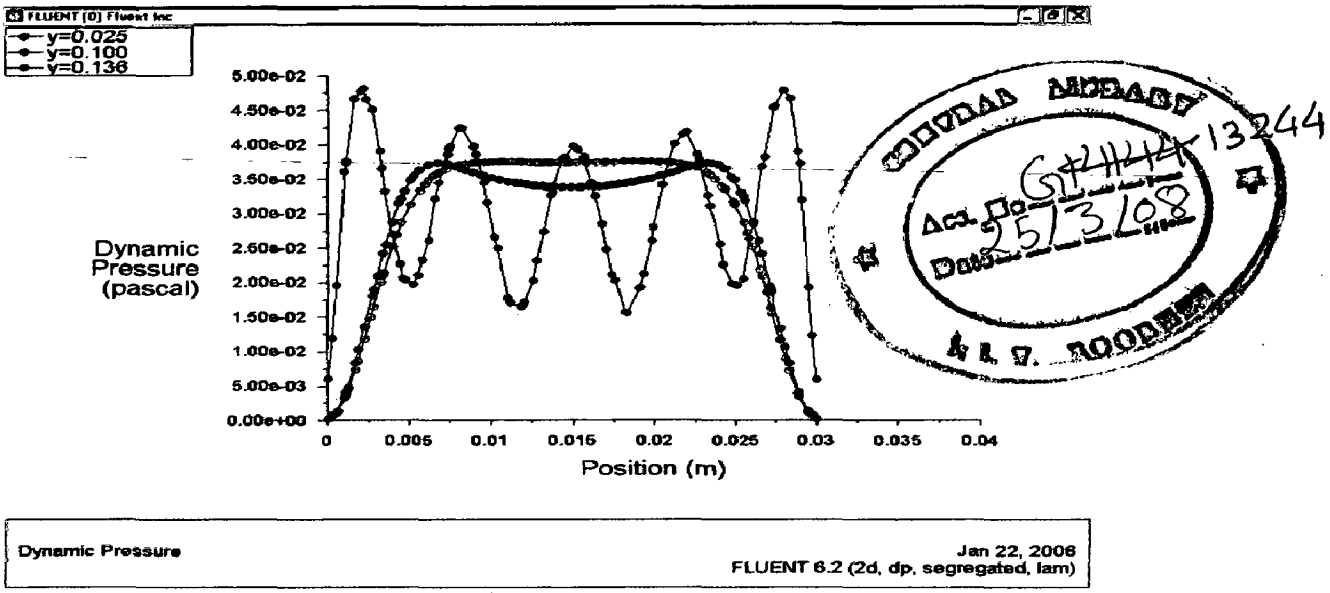

Fig.6.23 Pressure profiles for 101.325 kPa at different distances near particles

The pressure near the particles first increases and then it decreases throughout the diameter of the packed bed at Y=136 mm. At Y=25 mm the pressure is lower near the wall and higher at centerline of the bed. The similar pattern is observed at Y=100 mm but pressure at centerline in this case is higher than at it is Y=25 mm. The profiles are shown in Fig.6.23.

The pressure between the particles first increases and then it decreases throughout the diameter of the packed bed. The pressure increases between the wall and the adjacent particles and suddenly falls to the minimum value at the surface of the particle. The same nature of pressure is observed between the two adjacent particles. This phenomena is evident from the Fig.6.24, where the pressure profiles at Y=137.5 mm, Y=143.5 mm, Y=177.5 mm and Y=179 mm have shown. The pressure is lower in the case of Y=137.5 mm but for Y=143.5 to Y=179 the pressure is nearly similar.

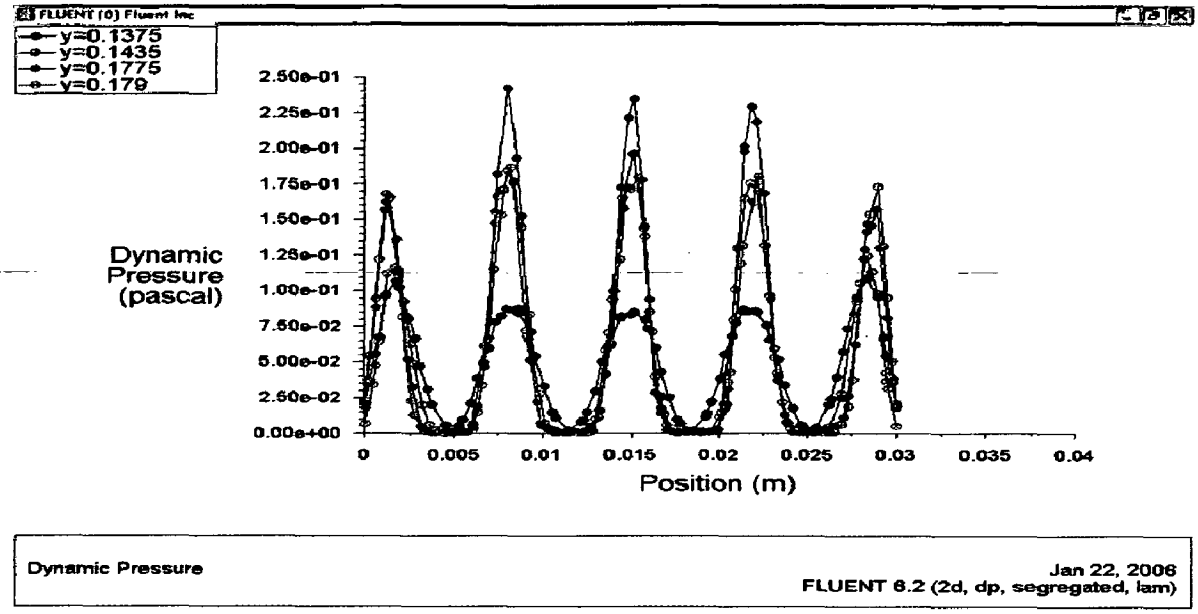

Fig.6.24 Pressure profiles for 101.325 kPa at different distances between particles

The pressure at Y=210 mm is higher in the center than the pressure at Y=250 mm but the pressure at Y=210 mm is varying and somewhat oscillating in nature. The pressure is uniformly distributed at the center of the packed bed at Y=250 mm. The pressure profiles are shown in the Fig.6.25.

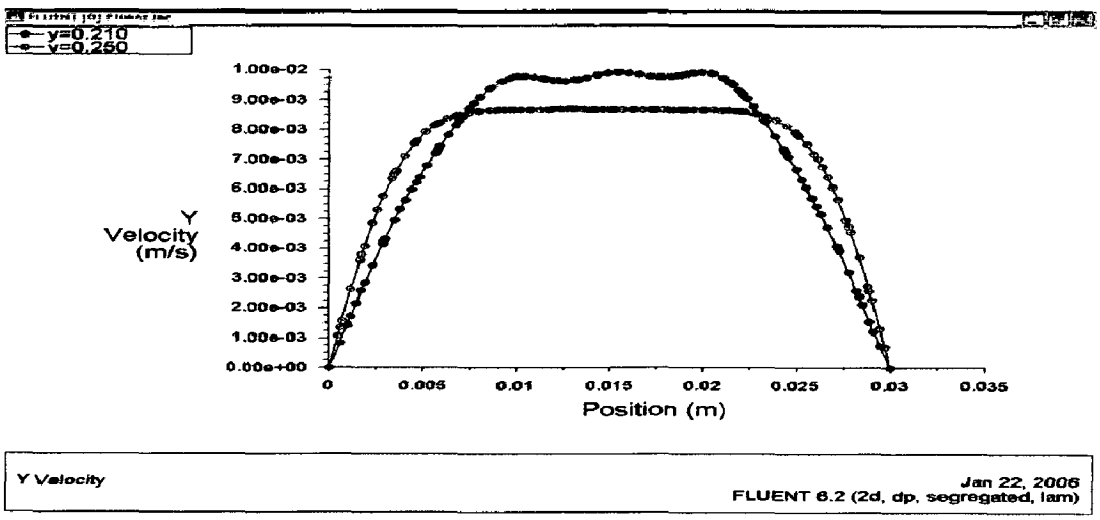

Fig.6.25 Pressure profiles for 101.325 kPa at different distances away from particles

6.3.2.3 Pressure profiles at 150000 Pa and at velocity of 9. 8 mm/s

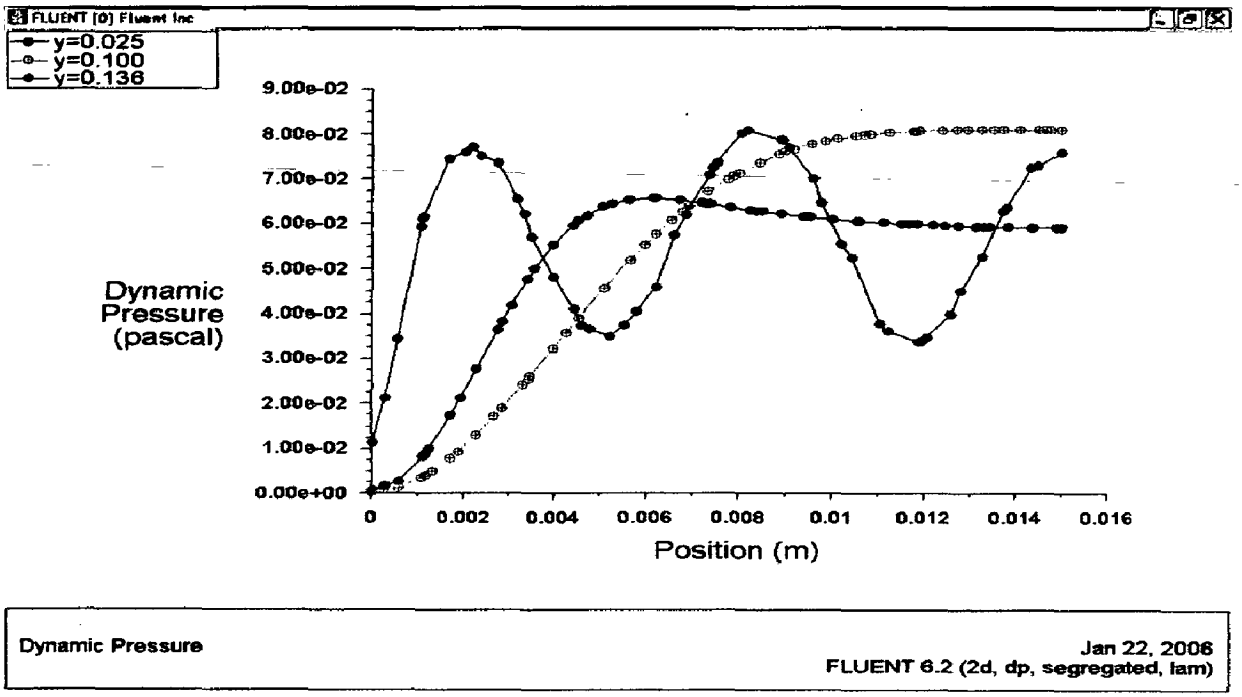

Fig.6.26 Pressure profiles for 150 kPa at different distances near particles

The pressure near the particles first increases and then it decreases throughout the diameter of the packed bed at Y=136 mm. At Y=25 mm the pressure is lower near the wall and higher at centerline of the bed. The similar pattern is observed at Y=100 mm but pressure at centerline in this case is higher than at it is Y=25 mm. The profiles are shown in Fig.6.26. The pressure at the center in the case for Y=100 mm becomes uniform.

The pressure increases between the wall and the adjacent particles and than falls to the minimum value at the surface of the particle. The same nature of pressure is observed between the two adjacent particles. This phenomena is evident from the Fig.6.27, where the pressure profiles at Y=137.5 mm, Y=143.5 mm, Y=177.5 mm and Y=179 mm have shown. The pressure is lower in the case of Y=137.5 mm but for Y=143.5 to Y=179 the pressure is nearly similar.

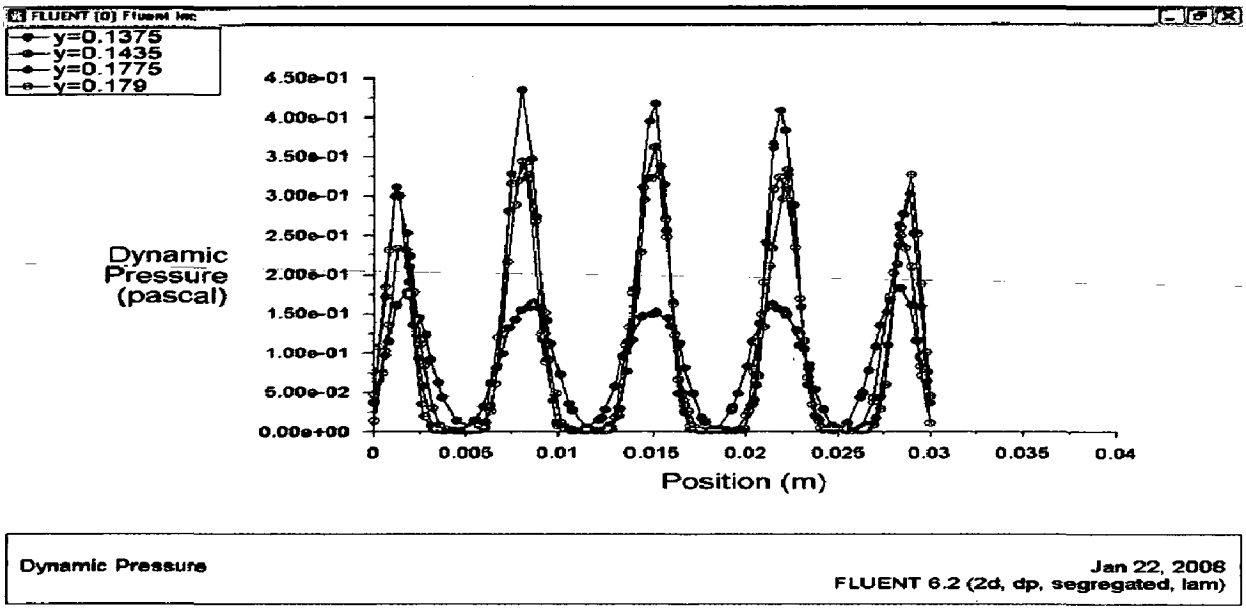

Fig.6.27 Pressure profiles for 150 kPa at different distances between particles

The pressure at Y=210 mm and at Y=250 mm are similar in the center but the pressure at Y=210 mm is varying and somewhat oscillating in nature. The pressure is parabolic in nature at the center of the packed bed at Y=250 mm. The pressure profiles are shown in the Fig.6.28.

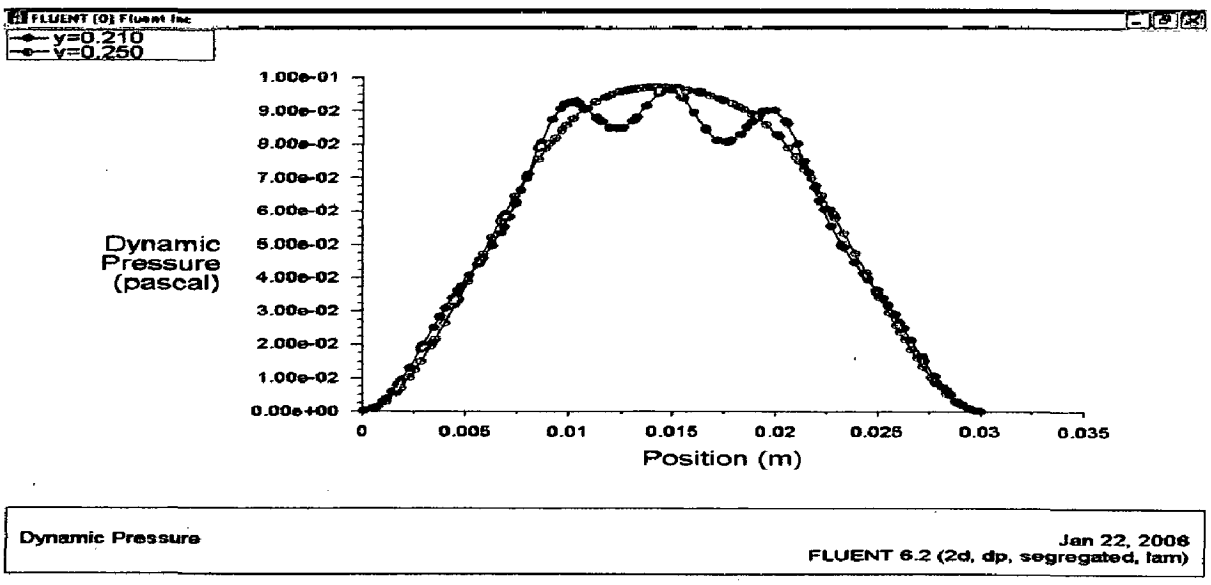

Fig.6.28 Pressure profiles for 150 kPa at different distances away from particles

6.4 Profiles of Velocity and Pressure for K-ε Model

Simulation of the packed bed is also done using K-ε Model to know the behavior of velocity and pressure under the influence of turbulence. For this purpose, different distances from the inlet of the packed bed at Y=30 mm, Y=100 mm, Y=136 mm, Y=143.5 mm, Y=177.5 mm, Y=0.179mm, Y=180 mm, Y=190 mm and Y=200 mm throughout the length of the packed bed variation in variables are plotted.

The simulation for K-ε model is done at pressure of 101325 Pa and at the velocity of 20.548 m/s and at the temperature of 300 K. The under relaxation factors used for various parameters are shown in the Table.

Parameters	Under Relaxation Factor (URF)
Pressure	0.2
Momentum	0.3
Turbulence kinetic energy	0.25
Turbulence kinetic dissipation rate	0.25
Turbulent viscosity	0.6

6.4.1 Profiles of Velocity

The variations in the velocity are measured at different distances along the length of the packed bed. The contour plot of the velocity along the length of the bed is shown in the Fig.6.29.

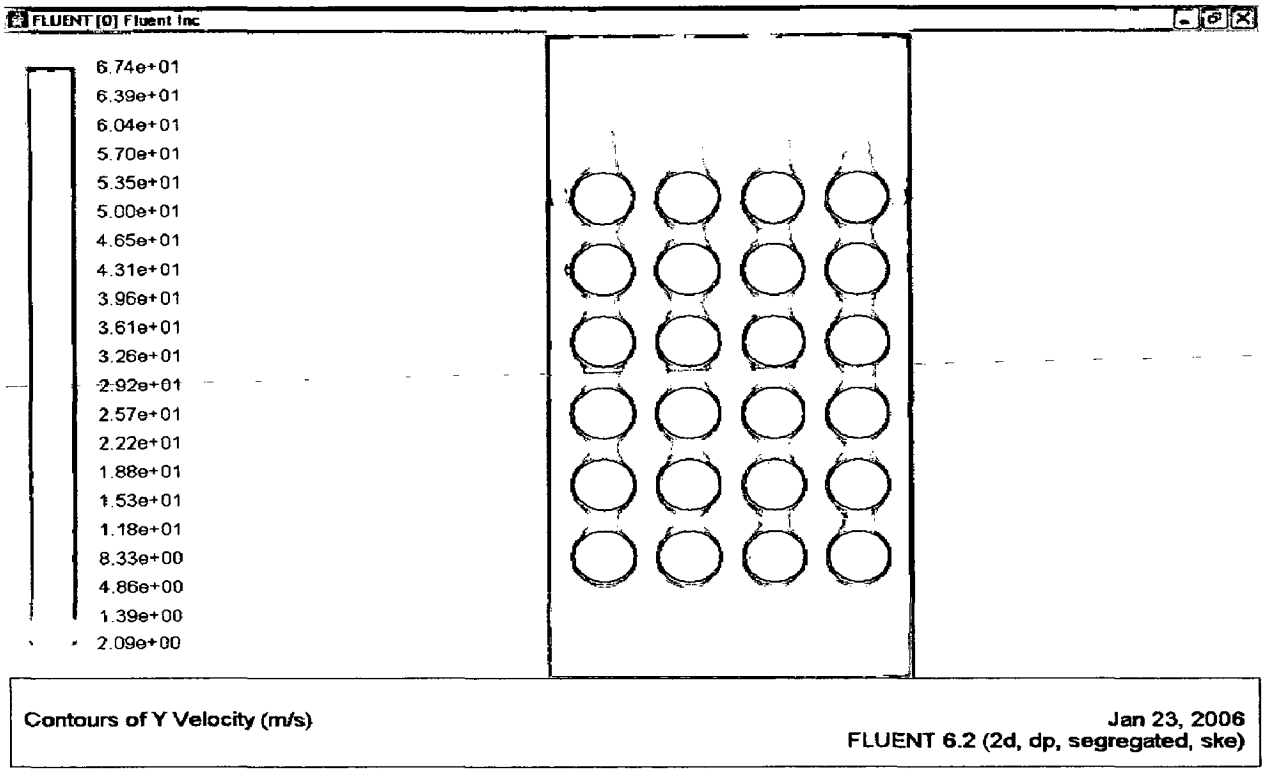

Fig.6.29 Contour of Velocity at 20.548 m/s

The velocity profiles near the particles at different distances from the inlet are shown in the Fig.6.30. The velocity at Y=30 mm and at Y=100 mm is similar and uniform at the center of the packed bed. The velocity profile at Y=136 mm is of

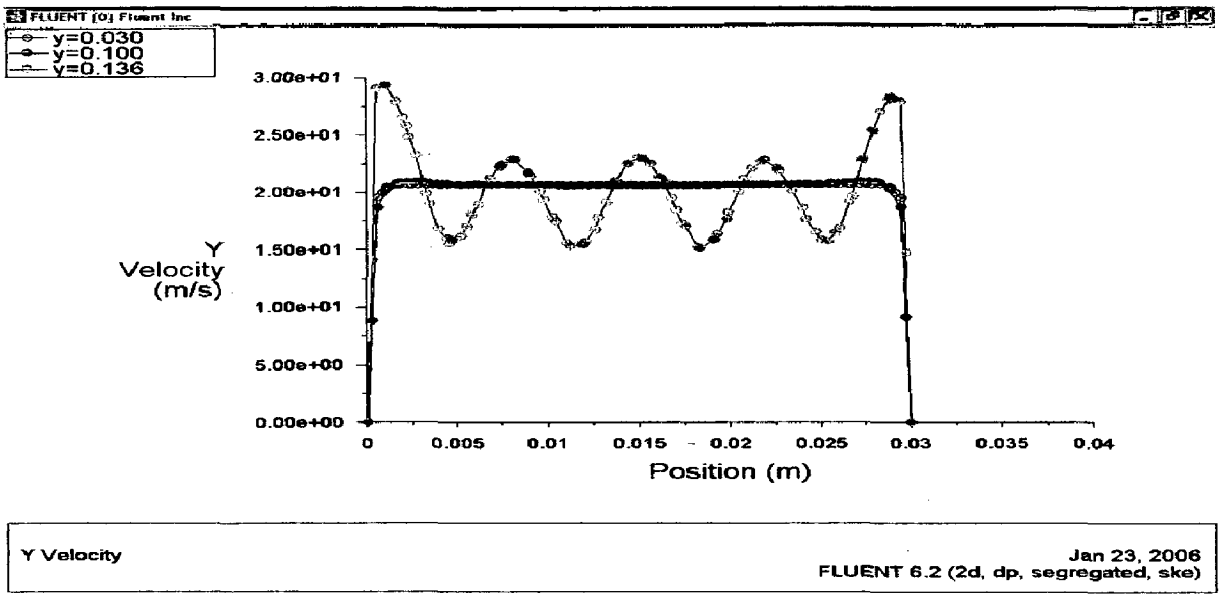

Fig.6.30 Profiles of Velocity at different distances near the particles

oscillating nature because of the influence of the spherical particles.

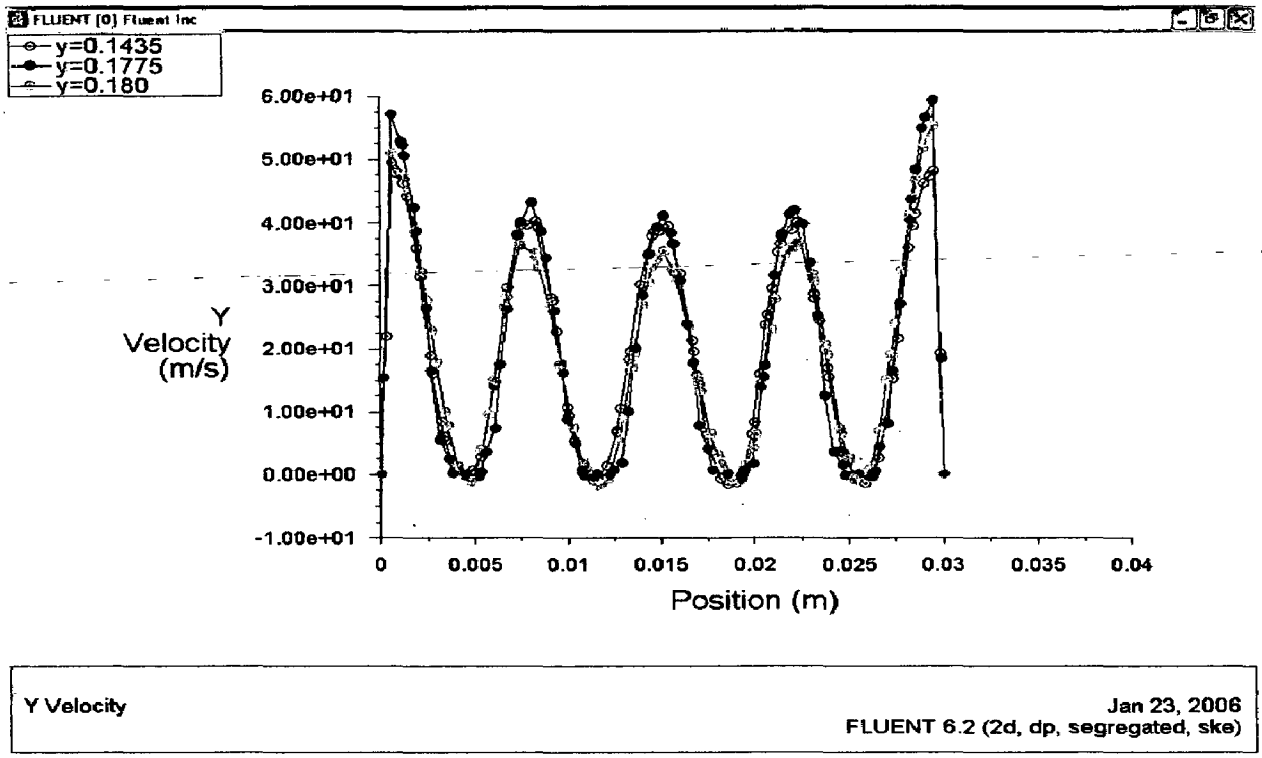

Fig.6.31 Profiles of Velocity at different distances between the particles

It can be seen from the fig.6.31 that the oscillation pattern of velocity has a similar tendency. The velocity has a zero value at the column wall, reaching the first peak value at 2.5 mm from the wall and has a minimum at 5 mm. The velocity at first peak for Y=143.5 mm is about 50 m/s and for Y=177.5 mm is about 57.5 m/s, this value of velocity is between wall and the particle near the wall. The velocity continues cycling with interval distance of peaks about 5 mm. The value of velocity at second peak for Y=143.5 mm is about 39 m/s and for Y=180 mm is about 35 m/s. The velocity at second peak is the velocity between two adjacent particles. The velocity near the particles is low and velocity between two adjacent particles is higher, it is obvious because between two adjacent particles the available area for the flow is much less and from the equation of continuity the velocity will increase. Consequently, the behavior of velocity is jet like between the particles and the value is much high than the free stream velocity.

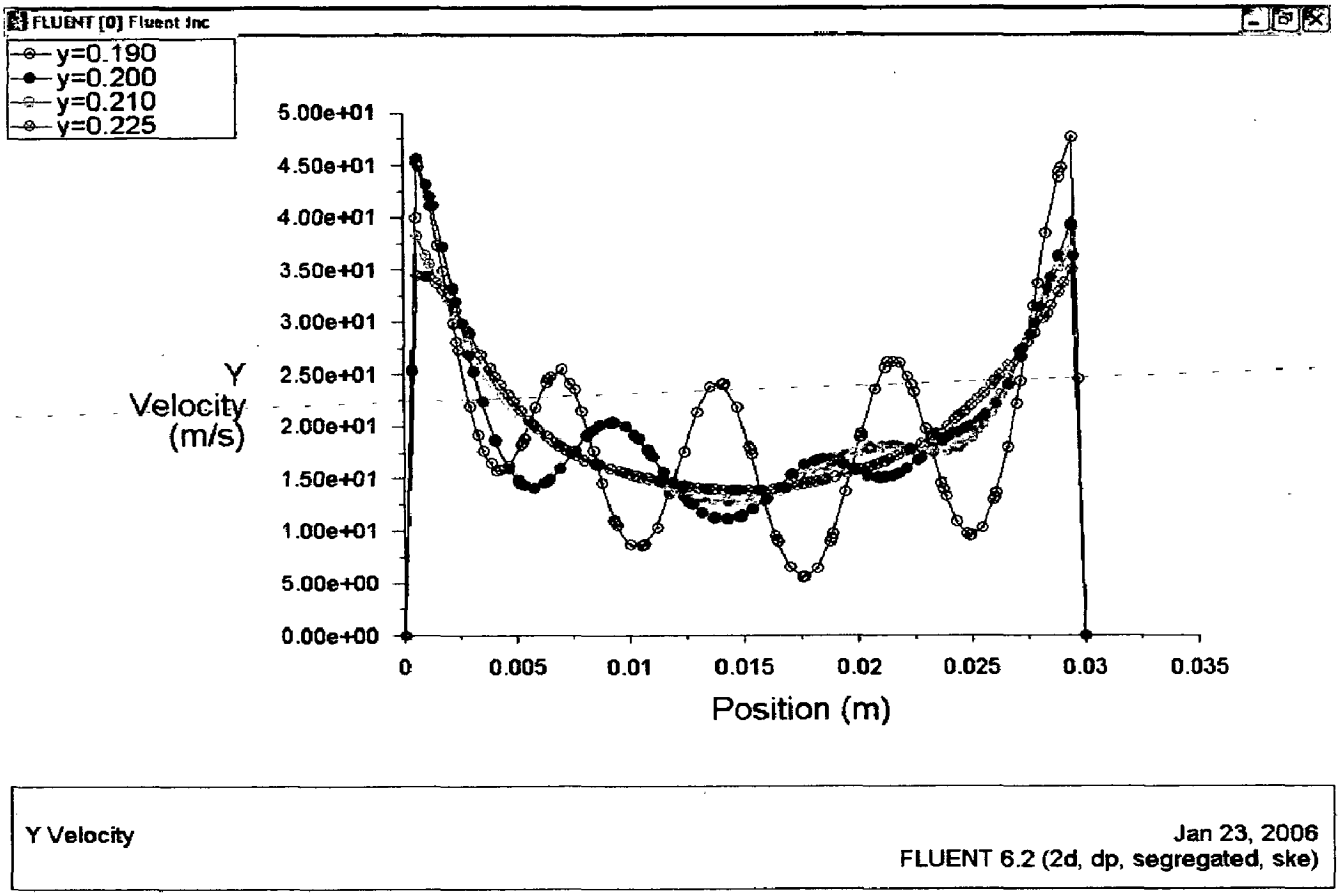

Fig.6.32 Profiles of Velocity at different distances away from particles

The velocity profiles away from the particles at different distances from the inlet shown in the Fig.6.32. At Y=190 mm and at Y=200 mm the profile of velocity are oscillating in nature and this oscillating pattern is gradually disappearing with respect to the distance. At Y=250 mm the velocity is decreasing and is of parabolic in nature.

6.4.2 Profiles of Pressure

The variations in the pressure are measured at different distances along the length of the packed bed. The contour plot of the pressure along the length of the bed is shown in the Fig.6.33

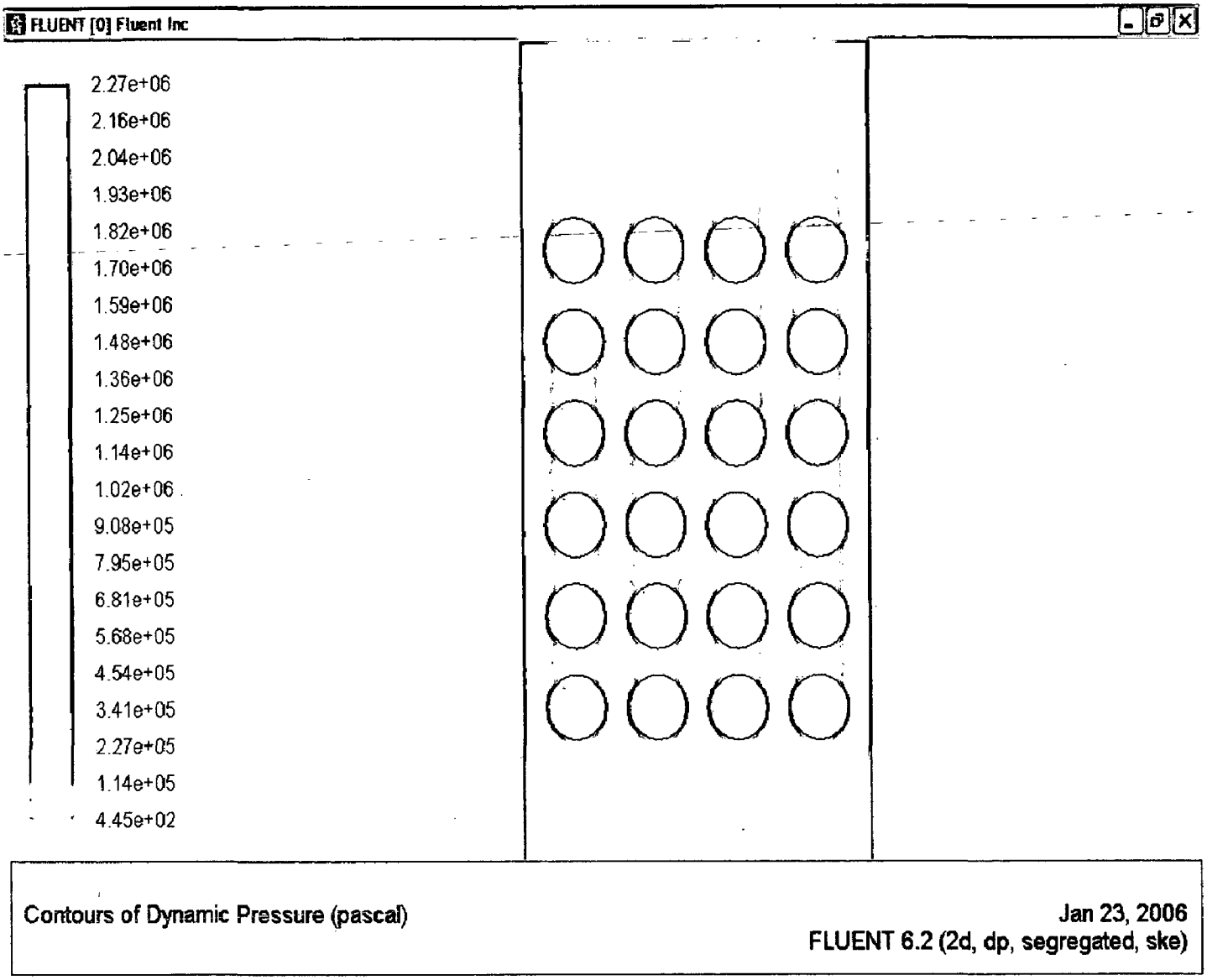

Fig.6.33 Contour plot of Pressure at 101325 Pa

From the Fig.6.32, it can be seen that the pressure between the wall and the adjacent particles and between the axially adjacent particles is much higher than the pressure between the vertically adjacent particles.

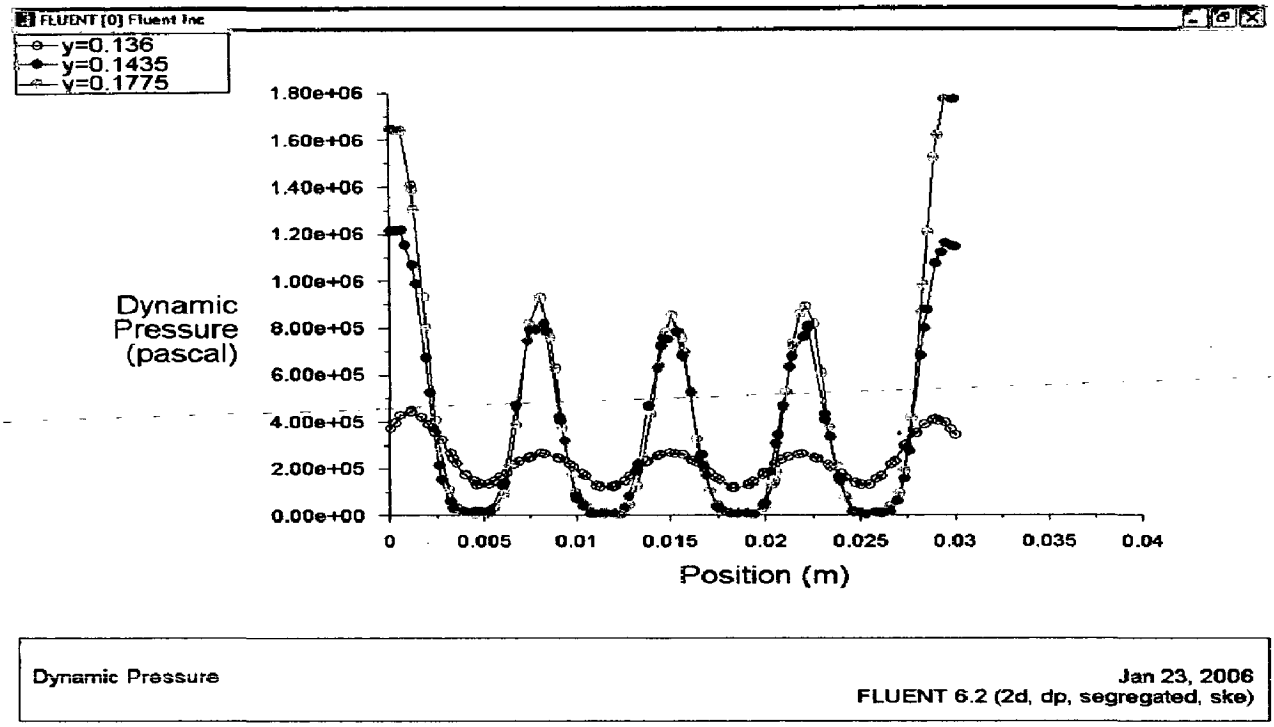

Fig.6.34 Pressure profiles at different distances between particles

The pressure between the particles and near the particles is of oscillating nature. But the pressure is nearly similar at Y=143.5 mm and at Y=177.5. the pressure at Y=136 mm of lower value.

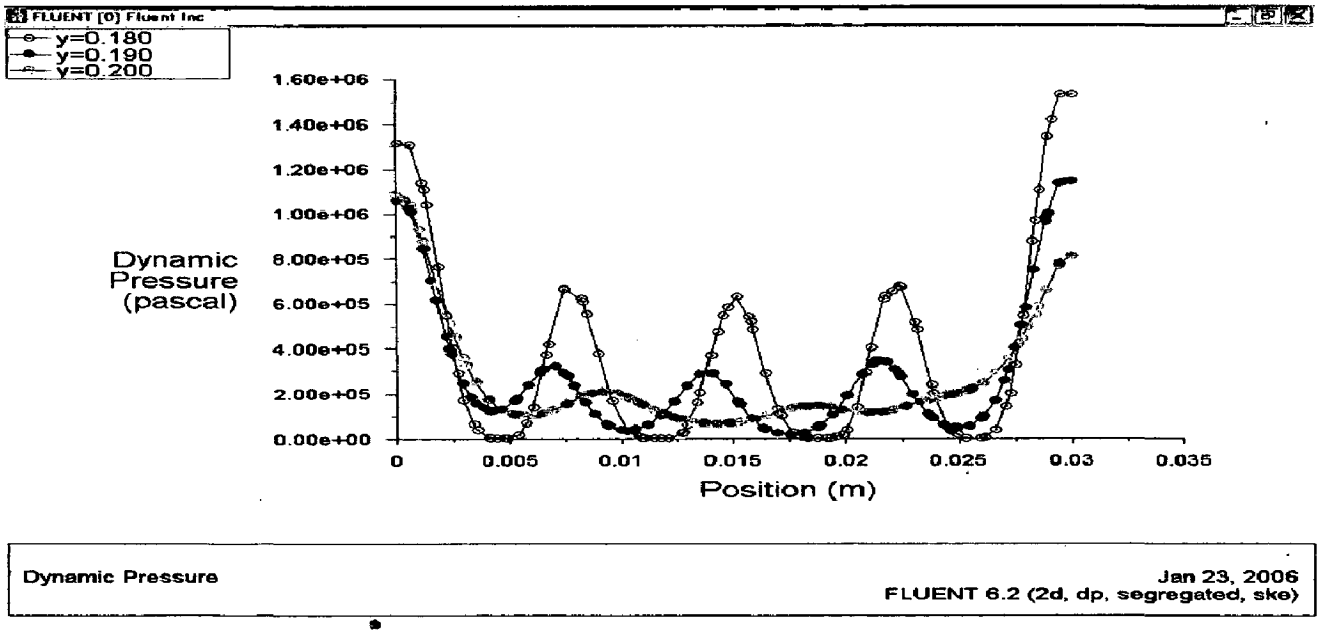

Fig.6.35 Pressure profiles at different distances away from particles

The pressure profiles away from the particles is still of oscillating nature but this nature of oscillation is disappearing with respect to the distance. It can be seen from the Fig.6.34 that at Y=180 mm the nature is oscillating and at Y=190 mm and Y=200 mm the oscillating pattern is becoming weaker and weaker gradually.

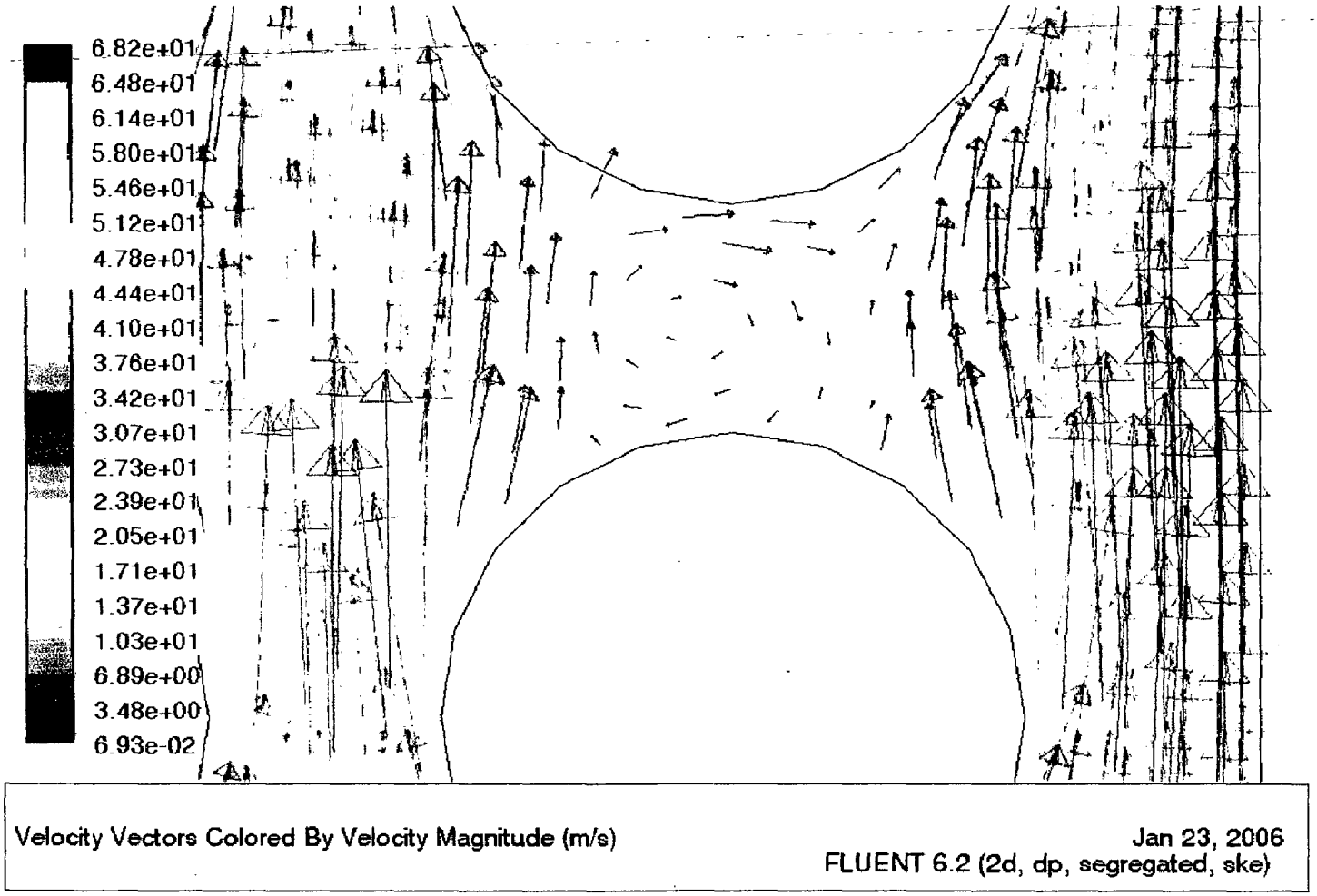

Fig.6.36 Eddies formation between two particles

The eddy formation between the two adjacent particles is shown in the Fig.6.35. It is clear from the fig. that eddies are stronger in turbulent case in comparison with laminar case, where eddies are not clearly formed.

CHAPTER – VII

CONCLUSION

Detailed measurements of water flow in a packed bed is generally difficult to accomplish because, behaviors at the boundaries of inlet of the packed bed can have a large effect on flow motion. It is necessary, therefore, to resolve at fine scale the behavior near surface and at the same time make measurements over the entire flow space.

This work approaches this measurement by taking readings at different distances with respect to length of the packed bed. The flows are modeled with a standard CFD numerical code FLUENT 6.2.16. Of the flow models examined, laminar model showed better than k- ε model.

Water velocity between the two adjacent particles is like a jet and is low in remaining part of the packed bed is predicted accurately. Pressure fluctuations are high between the wall and the adjacent particles and between the two adjacent particles. The pressure distribution is constant in the rest region of the bed which is free from the influence of the surface boundary of the particles.

The inlet region length of 140 mm is not sufficient to achieve parabolic flow profile for low inlet velocities except for 9.8 mm/s of inlet velocity.

CHAPTER – VIII

RECOMMENDATIONS FOR FUTURE WORK

In this dissertation the velocity profiles and pressure profiles are studied at steady state. In future the work can be extended to unsteady state or transient state.

In this thesis only one CFD package is used. Comparison can be done by taking simulation of same model in different packages like Fluent, CFX ,STAR CD etc.

In the present work 2d grid is considered for the study, in future the three dimensional grid can be developed and results can be compared.

Study for different size, different shapes ans different types of packings can be made in the future and and comparison can be made.

In this work water is used as a fluid, further work can be extended for the study of different types of fluids (liquids and gases).

Studies can further be extended for three phase system with continuous and discrete phases.

Studies for the reacting systems can be made in future.

This work can be further extended by refining the grid near the regions of spherical particles and comparison of results between both types of grids can be made.

REFERENCES

[1] Damjan Nemec and Janez Levec, "Flow through packed bed reactors: 1. Single-phase flow", Chemical Engineering Science (2005), vol 60, pp. 6947– 6957.

[2] Parsons I.M. and Porter K.E., "Gas flow patterns in packed beds: A Computational fluid dynamics model for wholly packed domains", Gas Separation & Purification (1992) ,Vol 6 No 4, pp. 1229 - 1236.

[3] Jiang Y., Khadilkar M.R., Al-Dahhan M.H., Dudukovic M.P, "CFD modeling of multiphase flow distribution in catalytic packed bed reactors: scale down issues", Catalysis Today (2001), vol 66, pp. 209–218.

[4] Subagyo, Standisht N. and Brookst G. A., "A new model of velocity distribution of a single-phase fluid flowing in packed beds", Chemical Engineering Science (1998), Vol. 53, No. 7, pp. 1375-1385.

[5] Higler A.P. and Krishna R., "CFD simulation of a structured packed column", Chemical Engineering Science (2004), vol 60, pp. 5843 – 5857.

[6] Arturo Ortiz-Arroyo, Faïçal Larachi, Bernard P.A. Grandjean and Shantanu Roy, "CFD Modeling and Simulation of Clogging in Packed Beds with non-Aqueous Media", AIChE J (2002), Vol 48, No. 8, pp. 1596-1609.

[7] Jiang Y., Khadilkar M.R., Al-Dahhan M.H., Dudukovic M.P., "Single phase flow modeling in packed beds: discrete cell approach revisited", Chemical Engineering Science (2000), vol 55, pp. 1829 - 1844.

[8] Latifi M.A, Lesage F. and Midoux N., "A two-zone model for liquid-to-wall mass transfer in a packed-bed reactor with single phase liquid flow", Computers chem. Engg (1998), Vol. 22, Suppl., pp. S905-S908.

[9] Natarajan S., Zhang C. and Briens C., "Numerical Simulation and Experimental Verification of Gas Flow through Packed Beds", Chemical Engineering Process (2003), vol 3, pp. 23-37.

[10] Lesage F. ,Latifi M.A and Midoux N., "Boundary element method in modelling of momentum transport and liquid-to-wall mass transfer in a packed-bed reactor", Chemical Engineering Science (2000) vol 55, pp. 455 - 460.

[11] Farcal Larachi, Catalin Florin Petre, Ion Iliuta and Bernard Grandjean, "Tailoring the pressure drop of structured packings through CFD simulations", Chemical Engineering and Processing (2003), vol 42, pp. 535 - 541.

[12] Coen van Gulijk, "Using computational fluid dynamics to calculate transversal dispersion in a structured packed bed", Computers Chem. Engg (1998), Vol. 22, Suppl., pp. Sl61-Sl70.

[13] Ortiz-Arroyo A. and Larachi F., "Lagrange–Euler–Euler CFD approach for modeling deep-bed filtration in trickle flow reactors", Separation and Purification Technology (2005), vol 41, pp. 155–172.

[14] Meisen Li, Yoshiyuki Bando, Takanori Tsuge, Keiji Yasuda and Masaaki Nakamura, "Analysis of liquid distribution in non-uniformly packed trickle bed with single phase flow", Chemical Engineering Science(2001), vol 56, pp. 5969–5976.

[15] Humby S. J., Biggs M. J. and Tuzun U., "Explicit numerical simulation of fluids in reconstructed porous media", Chemical Engineering Science(2002), vol 57, pp. 1955 – 1968.

[16] Prashant R. Gunjal, Vivek V. Ranade, and Raghunath V. Chaudhari "Computational Study of a Single-Phase Flow in Packed Beds of Spheres", American Institute of Chemical Engineers AIChE J, (2005), *Vol* 51, pp. 365–378.

[17] Tetsuya Suekane, Yasuo Yokouchi, and Shuichiro Hirai "Inertial Flow Structures in a Simple-Packed Bed of Spheres", AIChE Journal (2003), Vol. 49, pp. 2143 – 2154.

[18] Johns M. L., Sederman A. J., Bramley A. S., and Gladden L. F. "Local Transitions in Flow Phenomena through Packed Beds Identified by MRI", AIChE Journal (2000), vol 46, pp. 2151 – 2161.

[19] Michiel Nijemeisland and Anthony G. Dixon "CFD Study of Fluid Flow and Wall Heat Transfer in a Fixed Bed of Spheres", American Institute of Chemical Engineers AIChE J (2004), vol 50, pp. 906–921.

[20] YOU Changfu, QI Haiying and XU Xuchang "DRAG FORCE IN DENSE GAS-PARTICLE TWO-PHASE FLOW ", ACTA MECHANICA SINICA (2003), Vol.19, No.3, pp. 504 – 519.

[21] FLUENT Inc, 2003: "FLUENT 6.1 User's Guide", Digital Copy.

[22] Patankar, S. V., and Spalding, D. B., 1980: "Heat and mass transfer in boundary".

[23] H. K. Versteeg and W. Malalasekera 1995: "An Introduction to Computational Fluid Dynamics - The Finite Volume Method". Prentice Hall, London, 272 pp.

[24] www.cfdonline.com

[25] www.fluent.com